

# ETS Factors Regulate Vegf-Dependent Arterial Specification

Joshua D. Wythe,<sup>1,2,4,\*</sup> Lan T.H. Dang,<sup>5,6,7</sup> W. Patrick Devine,<sup>1,3,4</sup> Emilie Boudreau,<sup>5,6,7</sup> Stanley T. Artap,<sup>8</sup> Daniel He,<sup>1</sup> William Schachterle,<sup>4</sup> Didier Y.R. Stainier,<sup>4,9</sup> Peter Oettgen,<sup>8</sup> Brian L. Black,<sup>4</sup> Benoit G. Bruneau,<sup>1,2,4,\*</sup> and Jason E. Fish<sup>5,6,7,\*</sup>

<sup>1</sup>Gladstone Institute of Cardiovascular Disease, San Francisco, CA 94158, USA

<sup>2</sup>Department of Pediatrics

<sup>3</sup>Department of Pathology

University of California, San Francisco, San Francisco, CA 94143, USA

<sup>4</sup>Cardiovascular Research Institute, University of California, San Francisco, CA 94158, USA

<sup>5</sup>Toronto General Research Institute, University Health Network, Toronto M5G 1L7, Canada

<sup>6</sup>Department of Laboratory Medicine and Pathobiology, University of Toronto, Toronto M5S 1A8, Canada

<sup>7</sup>Heart and Stroke Richard Lewar Centre of Excellence in Cardiovascular Research, Toronto M5G 1L7, Canada

<sup>8</sup>Divisions of Cardiology and Molecular and Vascular Medicine, Center for Vascular Biology Research, Beth Israel Deaconess Medical Center, Harvard Medical School, Boston, MA 02215, USA

<sup>9</sup>Department of Developmental Genetics, Max Planck Institute for Heart and Lung Research, Bad Nauheim 61231, Germany

\*Correspondence: [jwythe@gladstone.ucsf.edu](mailto:jwythe@gladstone.ucsf.edu) (J.D.W.), [bbruneau@gladstone.ucsf.edu](mailto:bbruneau@gladstone.ucsf.edu) (B.G.B.), [jason.fish@utoronto.ca](mailto:jason.fish@utoronto.ca) (J.E.F.)

<http://dx.doi.org/10.1016/j.devcel.2013.06.007>

## SUMMARY

Vegf signaling specifies arterial fate during early vascular development by inducing the transcription of *Delta-like 4 (Dll4)*, the earliest Notch ligand gene expressed in arterial precursor cells. *Dll4* expression precedes that of Notch receptors in arteries, and factors that direct its arterial-specific expression are not known. To identify the transcriptional program that initiates arterial *Dll4* expression, we characterized an arterial-specific and Vegf-responsive enhancer of *Dll4*. Our findings demonstrate that Notch signaling is not required for initiation of *Dll4* expression in arteries and suggest that Notch instead functions as a maintenance factor. Importantly, we find that Vegf signaling activates MAP kinase (MAPK)-dependent E26 transformation-specific sequence (ETS) factors in the arterial endothelium to drive expression of *Dll4* and *Notch4*. These findings identify a Vegf/MAPK-dependent transcriptional pathway that specifies arterial identity by activating Notch signaling components and illustrate how signaling cascades can modulate broadly expressed transcription factors to achieve tissue-specific transcriptional outputs.

## INTRODUCTION

Arterial and venous blood vessels are anatomically, functionally, and molecularly distinct. Establishing and maintaining these separate endothelial cell fates is critical to the proper function of circulatory networks in the embryo and the mature adult (Marchuk, 1998). Angioblasts are specified in the lateral plate mesoderm during gastrulation. Bilateral streaks of vascular

endothelial growth factor receptor 2 (VEGFR2)/Flk1<sup>+</sup>-preaortic angioblasts, or arterial precursor cells (aPCs), form the dorsal aortae, followed by the formation of the embryonic veins by a distinct group of angioblasts (Chong et al., 2011). Arteriovenous (AV) specification is genetically determined before hemodynamic forces come into play. Hedgehog (Hh) signaling induces expression of Vegf in a dorsal to ventral gradient in the early embryo (Lawson et al., 2002). Arterial cells are thought to receive a higher concentration of Vegf, which activates p42/p44 MAPK signaling (Hong et al., 2006) and induces the expression and activation of Notch signaling pathway components exclusively in the arterial endothelium (Lawson et al., 2002). Once activated, the intracellular domain of the cleaved Notch receptor (NICD) interacts with its transcriptional cofactor, RBPJk, in the nucleus to induce expression of *Hey1/2*, *Hes1*, *EphrinB2 (Efnb2)*, and other downstream arterial genes (Yamamizu et al., 2010). The molecular events following Notch activation that maintain arterial identity are well understood (Swift and Weinstein, 2009), yet the initial transcriptional cues that function downstream of Vegf activation to induce the expression of Notch signaling components are unknown.

*Dll4* is the first Notch ligand gene expressed in the arterial endothelium (Chong et al., 2011), and its expression is induced by Vegf (Lawson et al., 2001). Expression of *Dll4* is initiated in the dorsal aorta before genes encoding its cognate receptors, *Notch1* and *Notch4*, making *Dll4* one of the earliest markers of the arterial lineage (Chong et al., 2011). Significantly, loss of only one copy of *Dll4* produces AV specification defects and embryonic lethality in mice (Duarte et al., 2004; Gale et al., 2004; Krebs et al., 2004). Defining the transcriptional program responsible for early *Dll4* expression will therefore provide key insights into arterial specification.

We describe the isolation of an arterial-specific enhancer of *Dll4*, which labels aPCs and differentiated arterial cells. We find that this enhancer is responsive to Vegf/MAPK signaling, and, through deletion analysis, we identify a previously unappreciated role for ETS transcription factors in mediating the

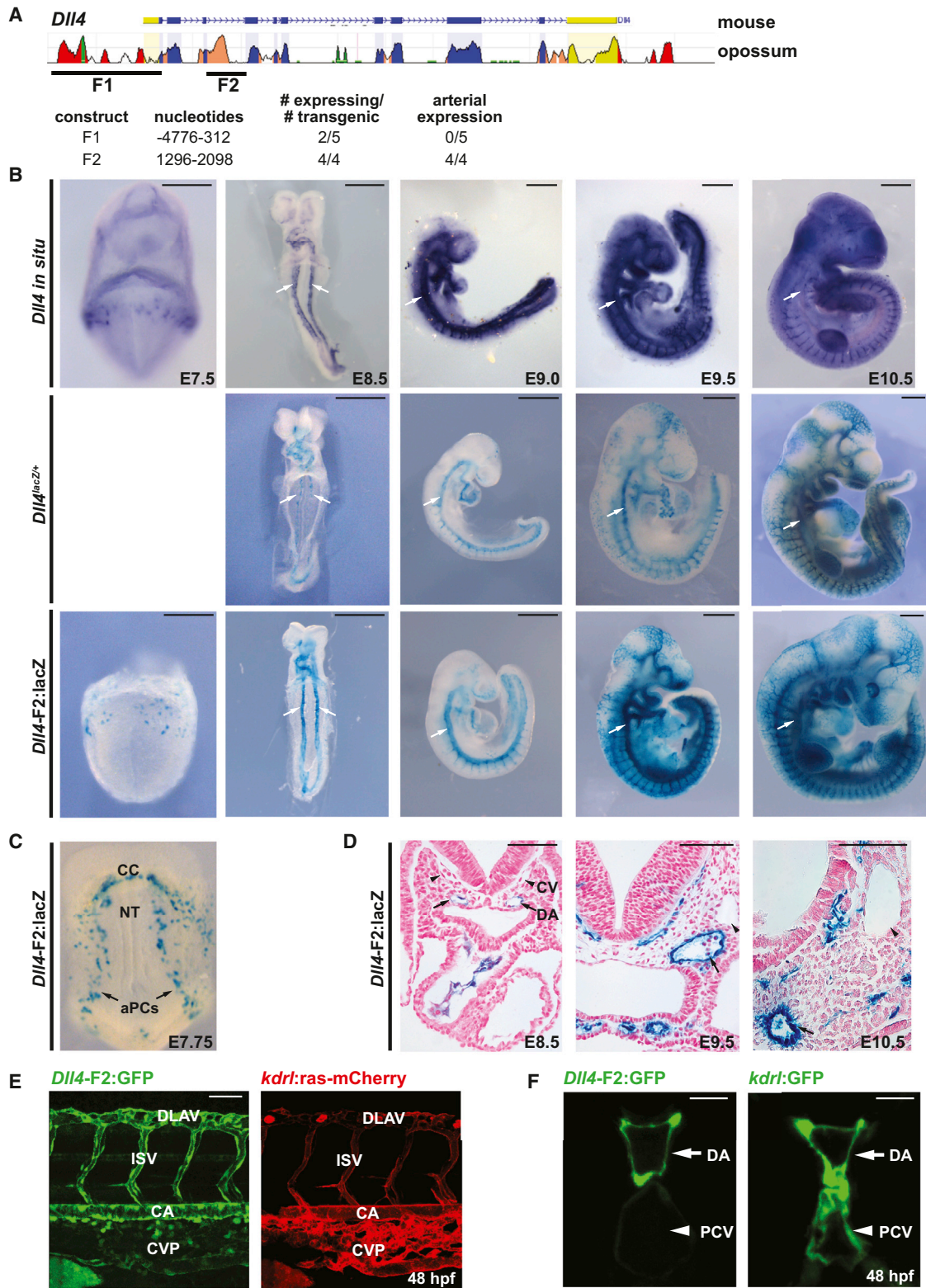


**Figure 1. Identification of an Intronic Enhancer of *Dll4* that Drives Arterial-Specific Expression**

(A) Conservation between murine and opossum *Dll4* with location of fragment 1 (F1) and F2 indicated. Transgenic analysis of F1-*lacZ* and F2-*hsp68-lacZ* (E9.5) is below. Further analysis of F1-*lacZ* is shown in Figures S1A and S1B.

(B) In situ hybridization of endogenous *Dll4* (top) and expression in *Dll4<sup>lacZ/+</sup>* (middle) and a stable *Dll4-F2-hsp68-lacZ* (F2) reporter line (bottom). Dorsal aorta (arrows).

(legend continued on next page)

Vegf-responsiveness and arterial-specificity of this enhancer and endogenous *Dll4*. This Vegf/MAPK/ETS pathway also regulates the expression of *Notch4*, which encodes an arterial-specific receptor of *Dll4*. These studies provide mechanistic insight into the transcriptional program downstream of the Vegf receptor that mediates arterial specification through the induction of Notch signaling components.

## RESULTS

### The Genomic Region 5' of *Dll4* Does Not Drive Arterial-Specific Expression

To understand the transcriptional basis of AV specification, we searched for evolutionarily conserved noncoding regions (ECRs) of the *Dll4* locus. The region proximal to the *Dll4* transcriptional start-site is regulated by  $\beta$ -catenin signaling through TCF/LEF sites and can also be activated by FOXC1/2 and RBPJK in vitro (Caolo et al., 2010; Corada et al., 2010; Seo et al., 2006). We cloned this 5-kb region (fragment 1, F1) and placed it upstream of a promoterless  $\beta$ -galactosidase reporter (Figure 1A; see also Figure S1A available online). The activity of this reporter construct was tested in transient transgenic mouse embryos, where it failed to direct any arterial expression (Figures 1A, S1A, and S1B). This suggests that this region is not sufficient to mediate the arterial-specific expression of *Dll4*.

### Wnt Signaling Is Not Required for Early *Dll4* Expression or Artery Specification

Endothelial-specific deletion of *Ctnnb1*, the gene encoding  $\beta$ -catenin, results in embryonic lethality at E12.5 (Cattellino et al., 2003). However, whether AV specification occurs normally in *Ctnnb1* loss-of-function mice has not been previously assessed. Overexpression of a dominant-active allele of *Ctnnb1* induces *Dll4* expression (Corada et al., 2010), leading to the suggestion that Wnt/ $\beta$ -catenin plays an instructive role in arterial specification by inducing Notch signaling. However, we were unable to detect active canonical Wnt signaling in the arterial endothelium at E8.5 or E9.5 using multiple established Wnt reporter lines (*BAT-gal*, *Axin2-d2EGFP*, *Axin2<sup>lacZ</sup>*) (Figures S1C–S1E). To determine if Wnt signaling regulates early *Dll4* expression, we ablated *Ctnnb1* specifically in the endothelium. The dorsal aortae and cardinal vein were morphologically normal at E8.5 (data not shown) and E9.5 (Figure S1F), expression of *Dll4* mRNA was unchanged (Figure S1G), and we did not observe any arteriovenous malformations (AVMs) in *Ctnnb1* mutants at E9.5 (Figure S1H). Collectively, these results demonstrate that Wnt/ $\beta$ -catenin signaling in the endothelium is dispensable for early artery formation and early *Dll4* expression and that the DNA region upstream of the promoter of *Dll4* is not sufficient for artery-specific expression.

### Identification of a *Dll4* Enhancer with Activity in the Developing Arterial Endothelium and Endocardium

Another well-conserved ECR (fragment 2, F2) is located within the third intron of *Dll4* (Figure 1A). This region can respond to FOXN4 (Luo et al., 2012), RBPJK/NICD, and  $\beta$ -catenin (Yamamizu et al., 2010) in both ex-vivo and in vitro reporter analyses, but its in vivo activity has not been assessed. In transient transgenic embryos, F2 drove robust activation of a minimal promoter-*lacZ* reporter (*hsp68-lacZ*) in the arterial endothelium and endocardium, similar to endogenous *Dll4* mRNA expression and to the  $\beta$ -galactosidase activity of *Dll4<sup>lacZ/+</sup>* embryos (Figure 1B). Analysis of embryos at E7.5–E7.75 from multiple stable transgenic founder lines demonstrated that this enhancer labeled aPCs prior to their coalescence into the cord-like structures of the dorsal aorta (Figures 1B and 1C). Examination of transverse sections confirmed the arterial-specificity of the enhancer from E8.5 through E10.5 (Figure 1D). F2 also drove strong expression in the endocardium, another tissue where *Dll4* mRNA is observed (Figure 1B), suggesting that this enhancer recapitulates the entire developmental endothelial expression pattern of endogenous *Dll4*. F2, like endogenous *Dll4*, was active in the arteries of the postnatal retina, but it was not active in the vasculature of the adult retina, suggesting that F2 is a developmentally regulated enhancer (data not shown). To determine whether this enhancer's functionality was conserved in other vertebrate species, we injected an F2:*GFP* transgene into zebrafish embryos and established stable transgenic lines. Expression of GFP was specific to the dorsal aorta, cardinal artery, and intersomitic vessels, with very little expression detectable in the posterior cardinal vein or caudal vein plexus (Figures 1E and 1F). This intronic *Dll4* F2 element is therefore a bona fide arterial-specific enhancer.

### A 36 bp Fragment Necessary and Sufficient for Arterial-Specific Enhancer Activity Is Regulated by ETS and RBPJK

Comparative genomic analysis revealed that the full-length F2 enhancer contains regions of high conservation among distantly related mammals (Figure 2A). Using deletion analyses of the 802 bp F2 enhancer, we identified a 350 bp (F2-2) and a 225 bp fragment (F2-4) that both labeled the arterial endothelium, as well as a weak endocardial enhancer (F2-3) that failed to label the arterial endothelium in mice (Figures 2A and 2B). The proximal 176 bp of the F2 enhancer (F2-5), which is contained in F2 and F2-2, but absent in F2-4, was not sufficient to drive arterial expression (Figures 2A and 2B). F2, F2-2, and F2-4 share a common 100 bp region that, when deleted in the context of the entire 802 bp enhancer (F2 $\Delta$ 1), abolished arterial activity (Figures 2A and 2B). A well-conserved 36 bp element within this common region was necessary (F2 $\Delta$ 2) and, when concatamerized head-to-tail in triplicate (F2-6(3X)), was sufficient to direct arterial and endocardial expression (Figures 2A–2C). Further characterization revealed that this minimal

(C) F2 expression in early arterial precursors (aPCs) and in cardiac crescent (CC). NT, neural tube.

(D) Transverse sections of F2 expression. DA, dorsal aorta (arrow); CV, cardinal vein (caret).

(E) A stable *Dll4*-F2-*E1b*:GFP transgenic zebrafish line demonstrates arterial-specific expression. *kdr*:*ras*-mCherry marks all blood vessels. CA, caudal artery; CVP, caudal vein plexus; ISV, intersomitic vessel; DLAV, dorsal longitudinal anastomotic vessel.

(F) Cross-section of axial vasculature of F2:*GFP* zebrafish. PCV, posterior cardinal vein. Scale bars represent 500  $\mu$ m (B), 100  $\mu$ m (D), 50  $\mu$ m (E), and 10  $\mu$ m (F). See also Figure S1.



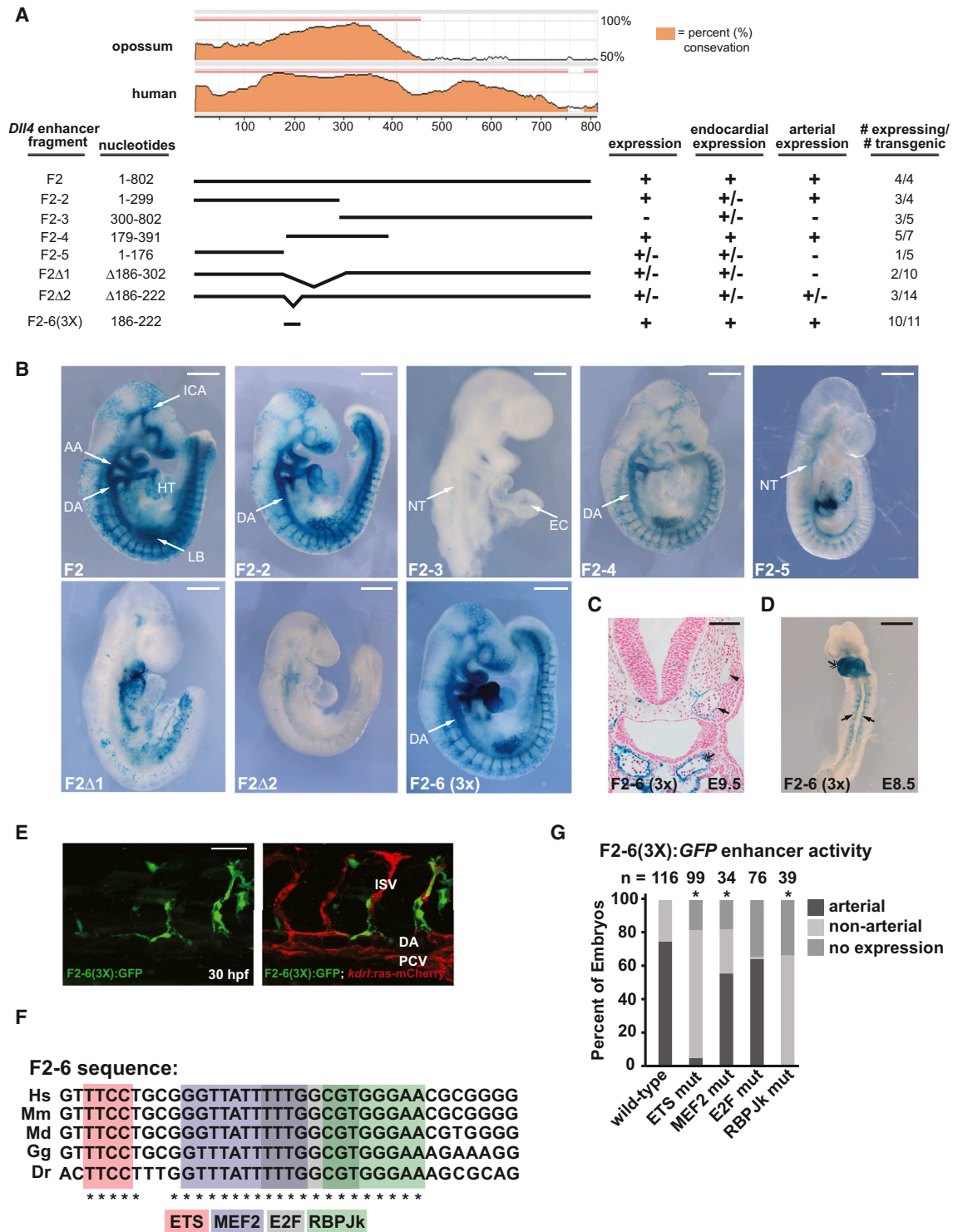


**Figure 2. Isolation of a Minimal *Dll4* Enhancer Element that Drives Arterial-Specific Expression**

(A) Sequence conservation of the F2 enhancer and deletion constructs used in transgenic analyses. Endocardial and arterial expression is indicated.

(B) Representative transgenic embryos from (A) at E9.5. F2, F2-2, and F2-4 directed strong arterial-specific expression. F2-3 directed weak endocardial (EC) expression. Deletion of a highly conserved 100 bp and 36 bp region (F2Δ1 and F2Δ2, respectively) abrogated arterial activity of the F2 enhancer. The 36 bp region, F2-6, was sufficient, when arrayed in triplicate, F2-6(3X), to direct arterial expression. DA, dorsal aorta; AA, aortic arch; LB, limb bud; NT, neural tube; ICA, internal cerebral artery; HT, heart.

(C) Transverse section of X-gal stained F2-6(3X)-lacZ embryo at E9.5. DA (arrow); cardinal vein (caret); EC (double arrow). Scale bar represents 100 μm.

(D) Whole-mount image of F2-6(3X)-lacZ embryo at E8.5. Scale bar represents 500 μm.

(legend continued on next page)



36 bp enhancer (F2-6(3X)) was capable of directing robust and reproducible arterial expression at early stages (i.e., E8.5) of vascular development (Figure 2D). Importantly, transient transgenesis revealed that this 36 bp enhancer was also able to drive strong arterial-specific expression in the dorsal aorta and intersomitic vessels (Figure 2E), as well as the endocardium (data not shown), of zebrafish embryos. Venous expression was not observed in embryonic mice or zebrafish (Figures 2C and 2E).

The minimal enhancer contains conserved predicted binding sites for ETS, MEF2, E2F, and RBPJk transcription factors (Figure 2F). We tested which sites were required for activity *in vivo* by separately mutating each DNA-binding site in the context of the F2-6(3X):GFP reporter and performing transient transgenesis assays in embryonic zebrafish. At 24 hr postfertilization (hpf), ~75% of embryos injected with the wild-type F2-6(3X) enhancer displayed arterial expression of GFP. Mutation of the E2F element did not affect enhancer activity, but mutation of the MEF2 element resulted in a modest, but significant reduction in arterial expression (Figure 2G). In mice, *Mef2a* and *Mef2c* are expressed within the endothelium (Lin et al., 1998; Wang et al., 2003) and loss of *Mef2c* leads to early embryonic lethality (~E9.5) and produces a range of vascular defects, including an absent or disorganized dorsal aorta (Bi et al., 1999; Lin et al., 1998). Although recombinant MEF2C protein bound to the MEF2 site of F2-6(3X) (Figure S2A), MEF2C was not required for either F2 activity or endogenous *Dll4* expression (Figures S2B and S2C). Conversely, only 5% of zebrafish embryos injected with an ETS mutant F2-6(3X):GFP construct had arterial expression and mutation of the RBPJk-binding site abolished arterial expression (Figure 2G). These results suggest that ETS and RBPJk play a critical role in regulating F2-6(3X) enhancer activity *in vivo* and imply that they may regulate endogenous *Dll4*.

#### Neither the RBPJk Site in the F2 Full-Length Enhancer nor Notch Signaling Are Required for Initiation of *Dll4* Expression

It has been proposed that activated Notch signaling can induce *Dll4* gene expression via RBPJk-mediated transcriptional regulation through a feed-forward mechanism (Caolo et al., 2010). Given that the activity of the minimal F2-6(3X) enhancer was dependent upon a putative RBPJk-binding site, we sought to determine if Notch signaling is necessary or sufficient to regulate the activity of the full-length F2 enhancer. Forced induction of Notch signaling throughout the vasculature promotes the arterialization of veins (Krebs et al., 2010). Indeed, endothelial-specific overexpression of the intracellular domain of Notch1 produced AVMs in mouse embryos and expanded F2 reporter activity into the venous endothelium (Figure S2D), suggesting that the enhancer is Notch responsive. However, although RBPJk bound to the F2 enhancer (Figure S2E), mutation of the RBPJk site in the context of the full-length F2 enhancer failed to diminish arterial-specific expression

in transient transgenesis analyses in zebrafish or mice (Figures 3A and 3B). We next assessed whether Notch signaling is required for F2 enhancer activity. *Rbpjk* knockdown in zebrafish reduced late (i.e., 26 hpf), but not early (i.e., 20 somites) enhancer activity (Figure 3C), consistent with a role for Notch signaling in the maintenance, but not the establishment of arterial *Dll4* enhancer activity. In mice, global loss of *Rbpjk*, which leads to defects in somitogenesis and neural tube formation (Oka et al., 1995), diminished but failed to abolish F2 reporter activity at E8.25 or E8.5 (Figure 3D). Additionally, in embryos where *Rbpjk* was ablated specifically in the endothelium—bypassing global morphogenetic defects—the activity of the F2 reporter was unaffected at E8.5 or E9.5 (Figure 3E), demonstrating that RBPJk does not play a cell-autonomous role in initiating *Dll4* enhancer activity. Finally, *Dll4* mRNA was only moderately reduced in *Rbpjk*<sup>-/-</sup> mice compared to wild-type littermates at E8.5 (Figure 3F). Together, these results indicate that Notch signaling is not required for the early arterial expression of *Dll4*, but is essential for its maintenance.

#### ETS Factors Regulate the Activity of the *Dll4* Enhancer

ClustalW analysis revealed the presence of nine perfectly conserved minimal ETS elements (ETS sites A–G), including the site within F2-6(3X) (ETS-B) (Figure S3A). This was intriguing because several ETS family members are key regulators of endothelial development (De Val and Black, 2009). EMSA confirmed that six of these sites competed for binding of the ETS1 DNA binding domain (DBD) to a known ETS element (Figure S3B). Among these six sites, ETS-B is present in all arterial-positive constructs (F2, F2-2, F2-4, and F2-6) and corresponds to a canonical ETS-1 binding site (cETS-1). ETS-B also directly and specifically bound recombinant ETS1-DBD (Figure S3C) and ETV2, an ETS family member (Figure S3D).

To determine the functional requirement of the ETS binding sites *in vivo*, we generated transient transgenic zebrafish harboring the full-length F2 enhancer driving GFP in which ETS-B or all six of the ETS1 DBD-binding ETS sites were mutated. Mutation of the six ETS binding sites abolished F2 enhancer activity, and mutation of the ETS-B site alone severely reduced enhancer activity in arteries (Figure 4A); confirming the importance of this single ETS element. Given the necessity of ETS binding sites for enhancer activity, we wondered whether ETS factors were sufficient to induce *Dll4* expression. Thus, we next determined whether overexpression of ETS factors was sufficient to induce expression of endogenous *DLL4* in human umbilical vein endothelial cells (HUVEC), a venous cell type that expresses low levels of *DLL4*. Indeed, overexpression of two different endothelial-enriched ETS family members, ETV2 or ERG, induced endogenous *DLL4* expression (Figure 4B). Induction of *DLL4* was accompanied by binding of V5-ERG to the endogenous region of *DLL4* corresponding to F2 (i.e., intron 3), but not to a distal region of the *DLL4* locus, as assessed

(E) Mosaic expression of F2-6(3x):GFP in the DA and intersomitic vessels (ISVs) of a transient transgenic 30 hpf zebrafish embryo. PCV, posterior cardinal vein. Scale bar represents 50  $\mu$ m.

(F) Sequence comparison of F2-6 in human (Hs), mouse (Mm), opossum (Md), chicken (Gg), and zebrafish (Dr). *Cis* elements are indicated.

(G) Each *cis* element was mutated in F2-6(3X):GFP and transient transgenics were assessed for arterial expression at 24 hpf. The percentage of embryos with expression in arteries (i.e., DA and/or ISV), expression elsewhere, and no expression, are indicated. Asterisk indicates a significant difference in arterial expression compared to wild-type ( $\chi^2$  test).

See also Figure S2.

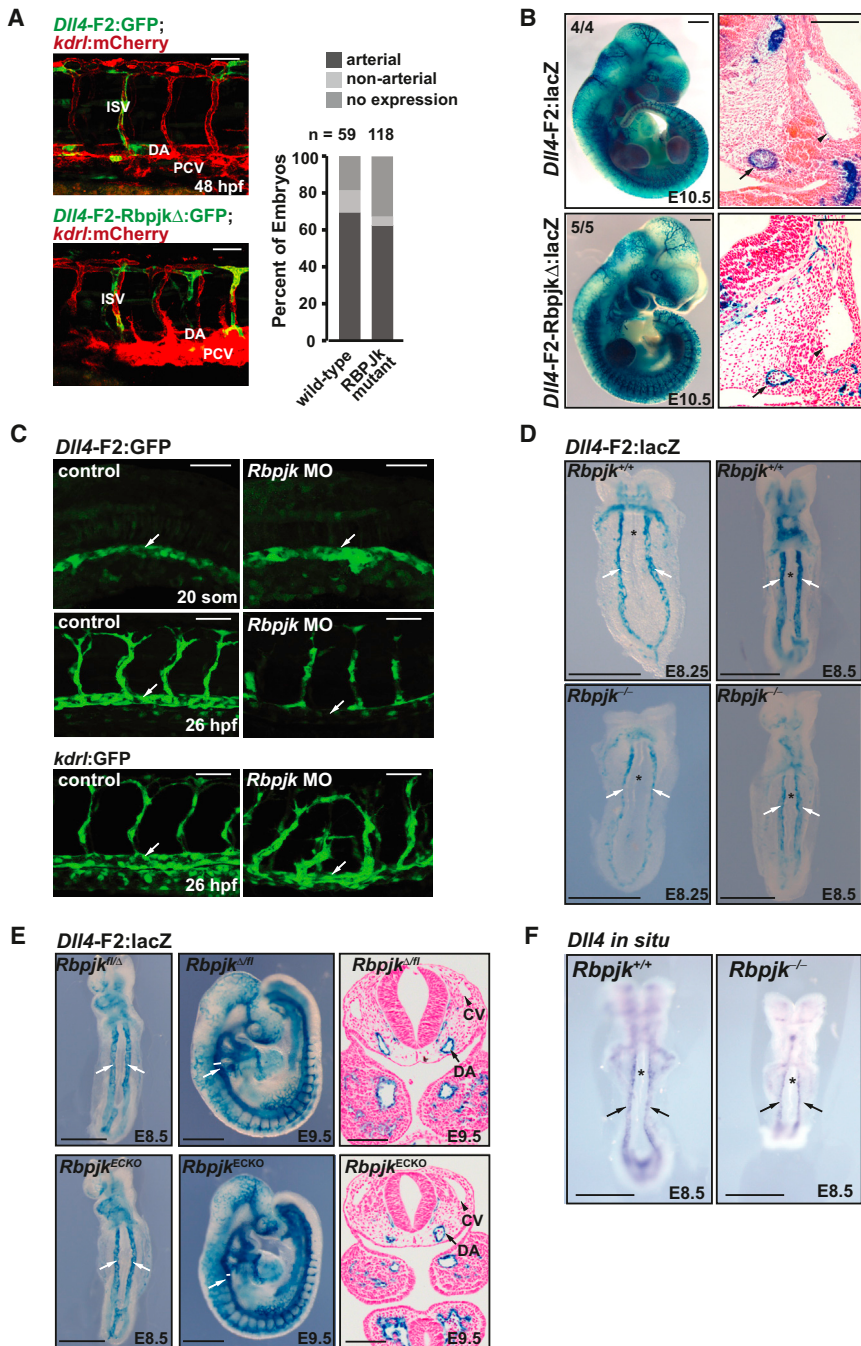


**Figure 3. Notch Signaling Is Not Required for Early Arterial Expression of *Dll4***

(A) Transient transgenesis of wild-type F2:GFP compared to a RBPJK mutant construct (F2ΔRBPJK:GFP). DA, dorsal aorta; PCV, posterior cardinal vein; ISV, intersomitic vessel.

(B) Whole-mount images (left), and transverse sections (right) of wild-type and RBPJK-mutated F2-lacZ transgenic embryos.

(C) Expression of F2:GFP in control and *rbpjk* morphant (MO) embryos, demonstrating normal enhancer activity in the DA (arrow) at 20 somites, but decreased expression at 26 hpf. Expression of *kdr*:GFP in the DA was unaffected.

(D) F2-lacZ expression was reduced but present in the DA of *Rbpjk*<sup>-/-</sup> embryos at E8.5 (*Rbpjk*<sup>+/+</sup>, n = 25; *Rbpjk*<sup>-/-</sup>, n = 5) and E8.25 (*Rbpjk*<sup>+/+</sup>, n = 14; *Rbpjk*<sup>-/-</sup>, n = 4).

(E) F2-lacZ expression was normal at E8.5 (left), and at E9.5 in whole-mount (center) and transverse sections (right) from embryos with endothelial cell-specific loss (ECKO) of *Rbpjk*, although mutants had a reduced DA diameter (bar) at E9.5, as previously reported (Krebs et al., 2004). E9.5, *Rbpjk*<sup>del/fli</sup>, n = 6; *Rbpjk*<sup>ECKO</sup>, n = 4; E8.5, *Rbpjk*<sup>del/fli</sup>, n = 8; *Rbpjk*<sup>ECKO</sup>, n = 3.

(F) In situ hybridization shows that *Rbpjk* is not absolutely required for *Dll4* expression at E8.5 (n = 3 for each genotype). DA, arrows; asterisk, neural tube. Scale bars represent 50 μm (A and C), 500 μm for whole-mounts, and 100 μm for sections (B and D–F).

See also Figure S2.

by chromatin immunoprecipitation (ChIP) (Figure 4C). Furthermore, we detected high levels of endogenous ERG occupancy at intron 3, but not a distal site in the *Dll4* locus, in an arterial cell line (bovine aortic endothelial cells [BAECs]) (Figure 4D). By comparison, NICD was only modestly enriched at intron 3 in BAECs (Figure 4D). Collectively, these results demonstrate that ETS factors can induce expression of endogenous *DLL4* mRNA and that ETS factors directly occupy the endogenous *DLL4* genomic region corresponding to F2 in arterial cells.

To further define the role of ETS factors in the regulation of *Dll4* expression, we performed loss- and gain-of-function experi-

ments in mouse and zebrafish. *Fli1a* and *Erg* are closely related ETS factors that play redundant roles in regulating angiogenesis during zebrafish vascular development (Liu and Patient, 2008). Combined morpholino knockdown of these two ETS factors decreased F2:GFP expression at both early and late stages of vascular development (Figure 4E), and endogenous *dll4*, *efnb2a*, and *hey2* expression were also diminished (Figure 4F). However, *kdr*:GFP expression (a pan-endothelial marker) was unaffected (Figure 4E), as was *kdr* mRNA (Figure 4F). Conversely, injection of *ERG* mRNA increased F2:GFP expres-

embryos (n = 83) compared to only 67% of *erg/fli1a* morphants (n = 165), suggesting that arterial Notch signaling was compromised in a proportion of ETS morphants (Figure 4G).

*Erg* splice variants in mice, driven from a translational start site in Exon 4, are specifically expressed in the endothelium, and *Erg Exon 4* null mouse embryos (*Erg*<sup>ΔEx4/ΔEx4</sup>) die early in development (E10.5–E11.5) with severe vascular remodeling defects in the yolk sac and impaired vascularization of the central nervous system (Vijayaraj et al., 2012). We found that the dorsal aortae formed normally in *Erg*<sup>ΔEx4/ΔEx4</sup> embryos (Figure S4B), but *Dll4* expression was modestly reduced at E8.5 (Figure 4H) and substantially downregulated at E9.5 (Figure 4I), confirming a role for this ETS family member in regulating *Dll4* mRNA expression. Interestingly, several other arterial markers were also reduced in *Erg*<sup>ΔEx4/ΔEx4</sup> embryos at E8.5 (Figure 4H), and levels of *Efnb2* were modestly reduced at E8.5 (Figures 4H and S4C) and E9.5 (Figure 4J), but were severely altered at E10.5 (data not shown). However, we did not find evidence of gross morphological AVM defects in *Erg*<sup>ΔEx4/ΔEx4</sup> embryos at E9.5 (Figures S4B and S4D) and only rarely observed shunts in *erg/fli1a* morphant zebrafish embryos (data not shown). We take these results to indicate that ETS factor redundancy may functionally compensate for the loss of ERG or Erg/Fli1a within the endothelium. Together these data define a role for ETS factors in the regulation of the arterial-specific expression of *Dll4* and indicate that ETS factors are involved in the specification of arterial fate.

### Vegf Signaling Regulates the Expression of *Dll4* through the Induction and Activation of ETS Factors

Arterial specification is largely Hh- and Vegf-dependent (Lawson et al., 2002; Vokes et al., 2004), and *Dll4* expression is regulated by Vegf levels (Coults et al., 2010; Liu et al., 2003). We therefore assessed whether F2 enhancer activity was Vegf-responsive. *vegfa* knockdown in zebrafish dramatically reduced F2 arterial enhancer activity (Figures 5A and 5B), similar to endogenous *dll4* mRNA (Figure 5C). However, the expression of a pan-endothelial marker (*kdr*:GFP) in the axial vessels and levels of *kdr* and *kdr1* mRNA were largely unaffected (Figures 5A–5C), confirming that *vegfa* does not regulate vasculogenesis in zebrafish. Global overexpression of Vegfa, achieved by coinjection of mRNAs encoding Vegfa<sub>121</sub> and Vegfa<sub>165</sub>, dramatically increased F2 activity in arterial cells (Figure 5D). In addition, F2 activity was expanded into the vein, confirming that Vegf levels regulate the arterial-specific expression of *Dll4*. Additionally, we examined F2-*lacZ* activity in two mutant mouse backgrounds that affect Vegf signaling. Hh-mediated activation of Smoothed (SMO) is required for expression of *Vegf* in the rostral somites at E8.5 and loss of *Smo* leads to disorganized or collapsed anterior (but not posterior) dorsal aortae by E8.5; although Fli1<sup>+</sup> cells are specified and present in normal numbers (Vokes et al., 2004). Significantly, *Smo* mutants have reduced *Dll4* mRNA in the anterior, but not posterior, dorsal aorta at E8.5 (Coults et al., 2010). Correspondingly, we found that F2 enhancer activity was reduced in the anterior, but not the posterior dorsal aorta of *Smo* mutants at E8.25, and activity was abolished in this region of the dorsal aorta by E8.5 (Figure S5A). Additionally, enhancer activity was absent in *Vegfr2*<sup>-/-</sup> embryos (Figure S5A), although this is likely the result of reduced vasculogenesis (Shalby et al., 1995).

To determine which *cis* elements within F2 mediate this Vegf responsiveness, we performed luciferase assays in cultured arterial endothelial cells treated with VEGF or the VEGF receptor inhibitor, SU5416. Endogenous *DLL4* mRNA was elevated in cells treated with VEGF compared to cells treated with SU5416 (Figure 5E). Although wild-type F2-*luciferase* activity was enhanced upon VEGF-treatment, mutation of ETS-B abrogated Vegf responsiveness and this reduction was only slightly more pronounced in the ETS-6x mutant (Figure 5F). Although mutation of the RBPJk site modestly reduced enhancer activity, this reduction was not as severe as mutation of the ETS elements. This suggests that the Vegf responsiveness of the *Dll4* enhancer is largely ETS-dependent.

Control of ETS activity by Vegf signaling could be mediated by alterations in the expression and/or activity of ETS factors. We first assessed whether the recruitment of ETS factors to the enhancer at the endogenous *DLL4* locus was dependent on Vegf signaling. RNA Polymerase II occupancy at the *DLL4* enhancer in cultured arterial cells was enhanced in VEGF-treated cells compared to cells treated with VEGF inhibitor (Figure 5G), a finding consistent with transcriptional regulation of *DLL4*. Importantly, ERG occupancy of the enhancer was also increased in the presence of Vegf signaling (Figure 5G). However, Vegf treatment did not alter ERG protein levels (Figure 5H), or ERG subcellular localization in arterial cells (Figures 5I and S5B). Interestingly, ERG protein levels were elevated in lysates from cells of arterial origin (human umbilical artery endothelial cells [HUAEC]) compared to corresponding venous cells (HUVEC) (Figure 5J), and expression of ERG was moderately enriched in the dorsal aorta compared to the cardinal vein in vivo (Figure S5C), suggesting that ERG is enriched in arterial cells. Although ERG levels were not affected by short-term inhibition of Vegf signaling in cultured arterial cells, the expression of several ETS factors are Vegf-responsive in vitro (Ghosh et al., 2012; Heo et al., 2010). Therefore, we examined the levels of endothelial-enriched ETS factors (Liu and Patient, 2008) to determine whether Vegf regulated their expression during vascular development. Compared to controls, quantitative RT-PCR (qRT-PCR) analyses revealed that levels of *elf2a*, *elf2b*, *elk4*, *erg*, *ets1a*, and *fli1a* were significantly reduced in *vegfa* morphants (Figures S5D and S5E). In contrast, the expression of *etv2*, which acts early in the gastrulation-stage mesoderm to specify endothelial cells (Lee et al., 2008), was unaffected by Vegf inhibition (Figures S5D and S5E). Thus, expression of several endothelial ETS factors is modulated by Vegf signaling in vivo, and their decreased expression coincides with a reduction in *dll4* expression.

To determine if ETS factors function downstream of Vegf signaling to induce *Dll4* expression, we overexpressed ERG in *vegfa* morphants. Coinjection of *ERG* mRNA partially rescued *Dll4* F2 enhancer activity, sprouting of ISVs, and endogenous *dll4* expression in *vegfa* morphant embryos (Figures 6A and 6B). Interestingly, F2 enhancer activity was expanded into the vein in ERG overexpressing *vegfa* morphants. Conversely, knockdown of *erg* and *fli1a* (using a subphenotypic dose of morpholino) prevented the Vegf-mediated induction of F2:GFP in both the artery and the vein (Figure 6C). Increased expression of endogenous *dll4* (Figure 6D) and *efnb2a* (Figure S6A) induced by Vegf overexpression was also blunted in *erg/fli1a* morphants. Collectively, our results show that Vegf regulates ETS factors in arterial endothelial



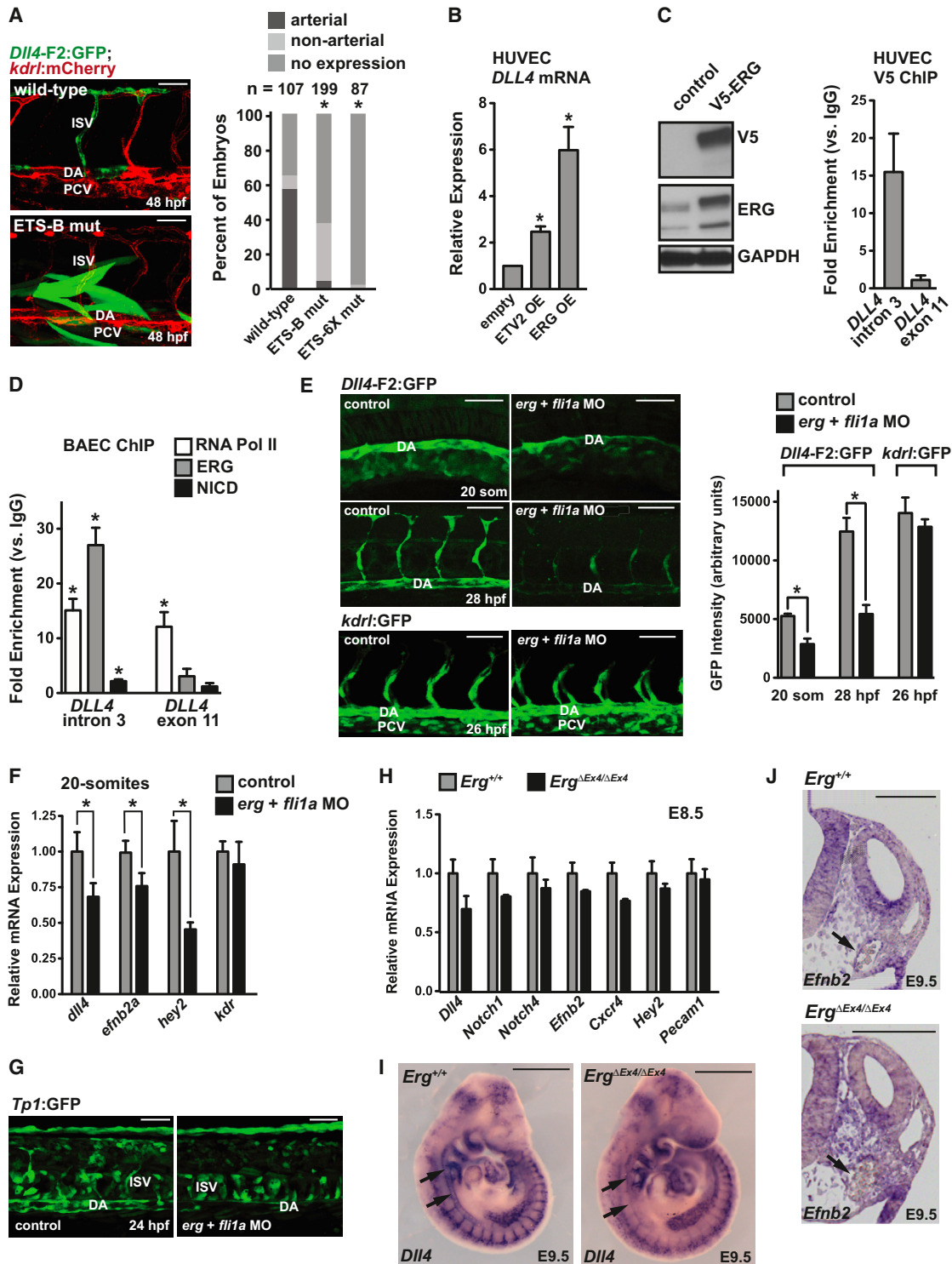


**Figure 4. *Dll4* Is Regulated by ETS Factors**

(A) Representative images (left) and quantification (right) of wild-type, ETS-B, and ETS-6x mutant F2:GFP embryos at 48 hpf. ISV, intersomitic vessel; DA, dorsal aorta; PCV, posterior cardinal vein. Asterisk indicates a significant difference in arterial expression compared to wild-type ( $\chi^2$  test).

(B) Expression of endogenous *DLL4* in HUVEC electroporated with *ETV2* or *ERG* expression constructs (n = 3, *ETV2*; n = 5, *ERG*).

(C) V5-ERG expression in electroporated HUVEC (left). ChIP in V5-ERG-electroporated HUVEC. Fold enrichment (V5 versus IgG) was measured at the *Dll4* enhancer (intron 3) and *Dll4* exon 11 (n = 2).

(D) ChIP in BAEC for RNA Polymerase II (RNA Pol II), ERG or the Notch intracellular domain (NICD) (n = 3). Asterisk indicates significant enrichment over IgG control.

(legend continued on next page)

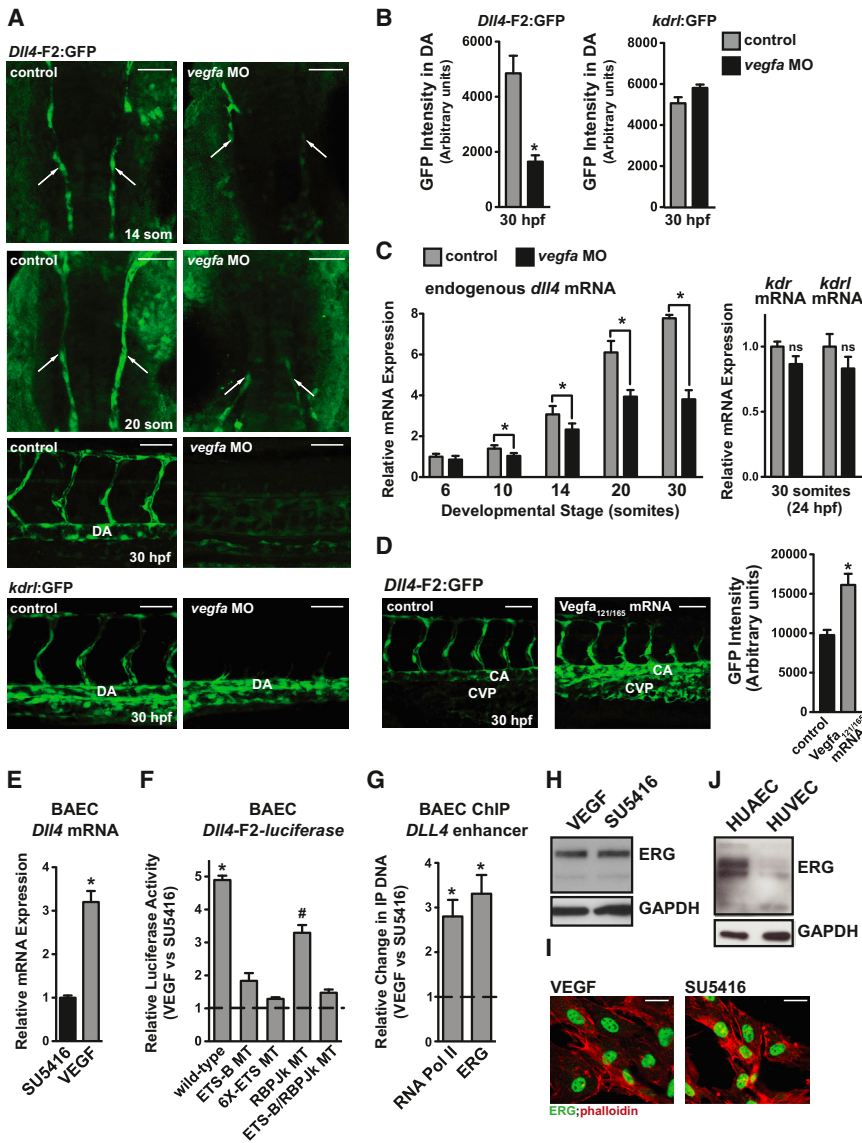


**Figure 5. Vegf Regulates the *Dll4* Enhancer through an ETS Element**

(A) Expression of F2:GFP (arterial) and *kdrl*:GFP (pan-endothelial) in control or *vegfa* morphant embryos. Lateral dorsal aorta (arrows); dorsal aorta (DA). Scale bar represents 50  $\mu$ m. (B) Quantification of GFP intensity in the DA ( $n \geq 10$  per group). (C) Expression (qRT-PCR) of *dll4* (arterial), *kdrl*, and *kdrl* (pan-endothelial) in control and *vegfa* morphant embryos ( $n \geq 3$  per group). (D) Overexpression of *Vegfa* enhanced expression of F2:GFP in arterial cells and expanded expression to venous cells. CA, caudal artery; CVP, caudal vein plexus. Quantification is shown ( $n = 6-8$  embryos per group). Scale bar represents 50  $\mu$ m. (E) Expression of *DLL4* (qRT-PCR) in BAECs treated with VEGF or VEGF receptor inhibitor (SU5416) for 24 hr ( $n = 3$ ). (F) Relative F2:Luciferase activity in BAEC treated with VEGF or SU5416. A representative experiment with three technical replicates is shown. Asterisk indicates a significant difference in luciferase activity compared to all other constructs. Number sign (#) indicates a significant difference between RBPJk MT and ETS-B MT, 6x-ETS MT and RBPJk/ETS-B MT. (G) ChIP assays for RNA Pol II and ERG in BAEC treated with VEGF or SU5416 for 24 hr ( $n = 3$ ). (H) Western blotting demonstrating equal expression of ERG protein in BAECs treated with VEGF or SU5416 for 24 hr. (I) Intracellular localization of ERG was unchanged by VEGF treatment. Scale bar represents 20  $\mu$ m. (J) Expression of ERG was elevated in arterial cells (HUAEC) compared to venous cells (HUVEC). All graphical data are mean  $\pm$  SEM. See also Figure S5.

cells by inducing their expression and recruitment to DNA. Vegf-regulated ETS factors in turn control F2 enhancer activity, endogenous *Dll4* expression and contribute to arterial specification.

**The Vegf/MAPK Pathway Activates an Arterial Transcriptional Program through Activation of ETS Factors**

Vegf-mediated activation of the p42/p44 MAPK and PI3K signaling pathways are known to promote or antagonize arterial

specification, respectively (Deng et al., 2013; Hong et al., 2006; Ren et al., 2010). Pharmacological inhibition of p42/p44 MAPK signaling in arterial cells in vitro decreased *DLL4* expression (Figure 7A). An arterial-enriched Notch receptor gene, *NOTCH4*, was also reduced, but *NOTCH1* and venous gene expression (*EPHB4* and *COUP-TFII*), were unchanged (Figure 7A). Consistent with decreased Notch ligand (i.e., *DLL4*) and receptor (i.e., *NOTCH4*) levels, expression of a Notch-activated transcription factor gene, *HES1*, and a Notch-dependent arterial marker, *EFNB2*, were also reduced (Figure 7A). These data suggest that MAPK signaling is required for the maintenance of Notch signaling in arterial endothelium. In contrast, inhibition of PI3K

(E) Expression of F2:GFP (arterial) and *kdrl*:GFP (pan-endothelial) in *erg;fli1a* morphants. Representative images (left) and quantification ( $n = 5-10$ ) (right). (F) Endogenous *dll4*, *ephrinb2a*, *hey2*, and *kdrl* in control and *erg;fli1a* morphants assessed by qPCR ( $n = 5-10$  individual embryos). (G) Notch activity (*Tp1*:GFP) was diminished in the dorsal aorta of ~30% of *erg;fli1a* morphants. (H) Levels of arterial markers and a pan-endothelial marker (*Pecam1*) were quantified by qRT-PCR in E8.5 embryos ( $n = 3$  for wild-type,  $n = 2$  for *Erg* <sup>$\Delta$ Ex4/  $\Delta$ Ex4</sup> embryos). (I) Endogenous *Dll4* mRNA is downregulated in the DA of *Erg* <sup>$\Delta$ Ex4/  $\Delta$ Ex4</sup> embryos (arrows;  $n = 3$  embryos per genotype) at E9.5. (J) *Efnb2* section in situ hybridization at 9.5 shows downregulation of *Efnb2* in the DA (arrows) of *Erg* <sup>$\Delta$ Ex4/  $\Delta$ Ex4</sup> embryos (*Erg*<sup>+/+</sup>,  $n = 3$ ; *Erg* <sup>$\Delta$ Ex4/  $\Delta$ Ex4</sup>,  $n = 2$ ). Scale bars represent 50  $\mu$ m (A, E, and G), 500  $\mu$ m (I), 100  $\mu$ m (J). All graphical data are mean  $\pm$  SEM. See also Figures S3 and S4.

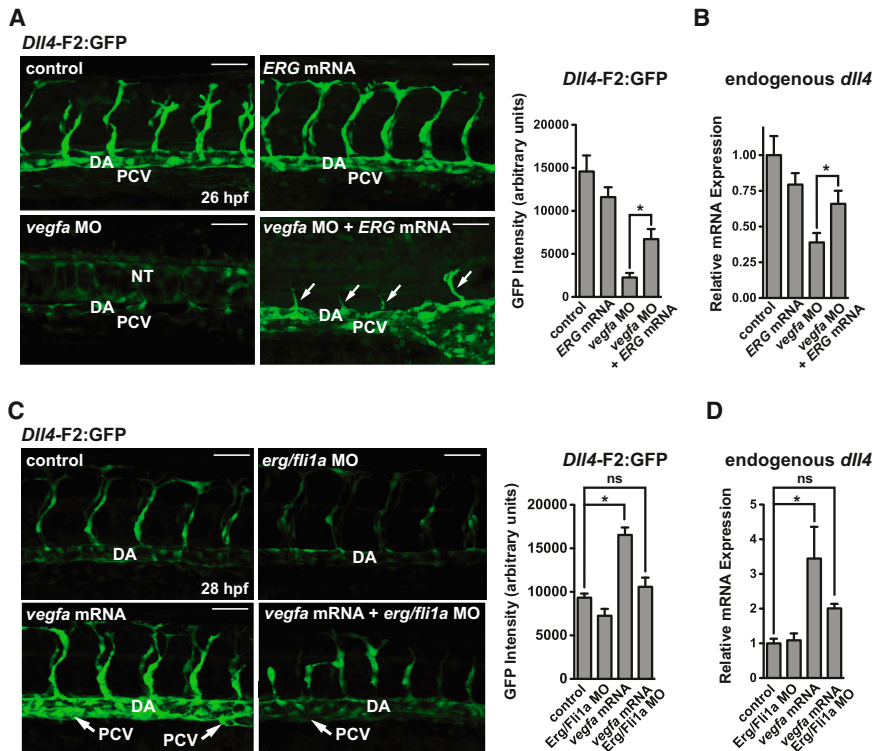


**Figure 6. ETS Factors Act Downstream of Vegf to Induce *dll4* Expression**

(A) *ERG* mRNA (200 pg) injection partially rescued F2:GFP expression and sprouting (arrows) in *vegfa* morphants at 26 hpf. Representative images (left) and quantification (right,  $n = 10-12$ ). (B) *dll4* mRNA expression (normalized to *kdr* expression) was assessed by qRT-PCR in individual 26 hpf embryos injected with *ERG* mRNA and/or *vegfa* morpholino ( $n = 4$ ).

(C) Partial knockdown of *erg* and *fli1a* with a subphenotypic dose of morpholino inhibited the induction of F2:GFP expression in both the dorsal aorta (DA) and posterior cardinal vein (PCV) in *Vegfa*<sub>121/165</sub> mRNA-injected embryos. Arrows indicate collapsed PCV. Quantification of 10-13 embryos per group is shown.

(D) Endogenous *dll4* mRNA was assessed by qRT-PCR in individual embryos at 24 hpf ( $n = 5$ ). All graphical data are mean  $\pm$  SEM. See also Figure S6A.

autonomous role for MAPK signaling in the regulation of arterial *Dll4* expression.

## DISCUSSION

Hh/Vegf-dependent activation of *Dll4* expression and Notch/RBPJk activity is a prerequisite for early artery specification and maintenance in the developing vertebrate embryo (Swift and Weinstein, 2009). The MAPK pathway activates the arterial program downstream of VEGFR2, whereas PI3K signaling antagonizes the MAPK pathway and arterial fate (Deng et al., 2013; Hong et al., 2006; Ren et al., 2010). However, the transcriptional mediators that are activated downstream of VEGFR2/MAPK and induce *Dll4* expression, and hence Notch activation, remain unknown. Here, we report the identification of an arterial-specific enhancer (F2) of *Dll4*, one of the earliest markers of the coalescing aPCs that form the dorsal aortae. The activity of the *Dll4* F2 enhancer described here recapitulates endogenous *Dll4* expression in the arterial and endocardial endothelium of the developing embryo. Functional analysis of this enhancer reveals that a minimal 36 bp DNA element, when concatenated, can drive arterial-specific expression, and through systematic mutation of the *cis* elements in this enhancer, we identify a role for the ETS family of transcription factors in the Vegf- and MAPK-dependent initiation of *Dll4* expression (Figure 7H). Critically, *Notch4* is also regulated by this Vegf/MAPK/ETS pathway, suggesting that this genetic network may coordinately activate expression of Notch signaling components to initiate Notch signaling in the early artery.

Previous work implicated FOXC1/2 and  $\beta$ -catenin in the regulation of *Dll4* expression (Corada et al., 2010; Seo et al., 2006; Yamamizu et al., 2010). However, our results argue against these factors directing the arterial-specific expression of *Dll4*. In the case of *Foxc1/2*-dependent regulation of *Dll4*, the conclusions rely largely upon the phenotype of *Foxc1*<sup>-/-</sup>;*Foxc2*<sup>-/-</sup> mice, which have AVMs and reduced arterial gene expression. However, these embryos also completely lack somites 1-8 at E8.5 (Seo et al., 2006), which are a critical source of Hh-induced

activity with the small molecule, LY29004, enhanced expression of *DLL4*, *NOTCH4*, *HES1*, and *EFNB2* (data not shown). Because *NOTCH4* was regulated similarly to *DLL4*, we examined ECRs within the *NOTCH4* locus for conserved ETS elements. An ECR within intron 1 of *NOTCH4* contained multiple conserved ETS sites, and this region had high ERG occupancy in arterial cells, as assessed by ChIP (Figure 7B). Overexpression of ERG in HUVEC induced *NOTCH4* mRNA, suggesting that *NOTCH4* is an ETS factor-regulated gene (Figure 7C). Similar to *DLL4*, *NOTCH4* expression was downregulated upon Vegf inhibition (Figure 7D), and this was accompanied by a decrease in ERG recruitment to intron 1 (Figure 7E). We also found that ERG recruitment to *DLL4* intron 3 and *NOTCH4* intron 1 was reduced in cells treated with a MAPK inhibitor (Figure 7F), suggesting that ERG recruitment to these enhancers is MAPK-dependent. Accordingly, Vegf-induced *Dll4* F2-luciferase activity was suppressed by MAPK inhibition in arterial cells and mutation of the ETS-B site largely abrogated this responsiveness (Figure 7G). In contrast, inhibition of PI3K signaling enhanced Vegf-induction of F2-luciferase activity, and this was also dependent on the ETS-B site (Figure S6B), suggesting that PI3K inhibition may enhance ETS activity. To determine whether MAPK regulates *Dll4* in vivo, we inhibited MAPK signaling beginning at the 10-somite stage and found a significant decrease in F2:GFP expression at 28 hpf (Figures S6C and S6D). Expression of endogenous *dll4* and *hey2* mRNA was also reduced, whereas *efnb2a* levels were modestly decreased (Figure S6E). However, *kdr*:GFP and *kdr* expression were unaffected (Figures S6D and S6E). In agreement with the MAPK inhibitor data, overexpression of dominant active MEKK in endothelial cells resulted in ectopic expression of F2:GFP within venous cells in vivo (Figure S6F), implying a cell-



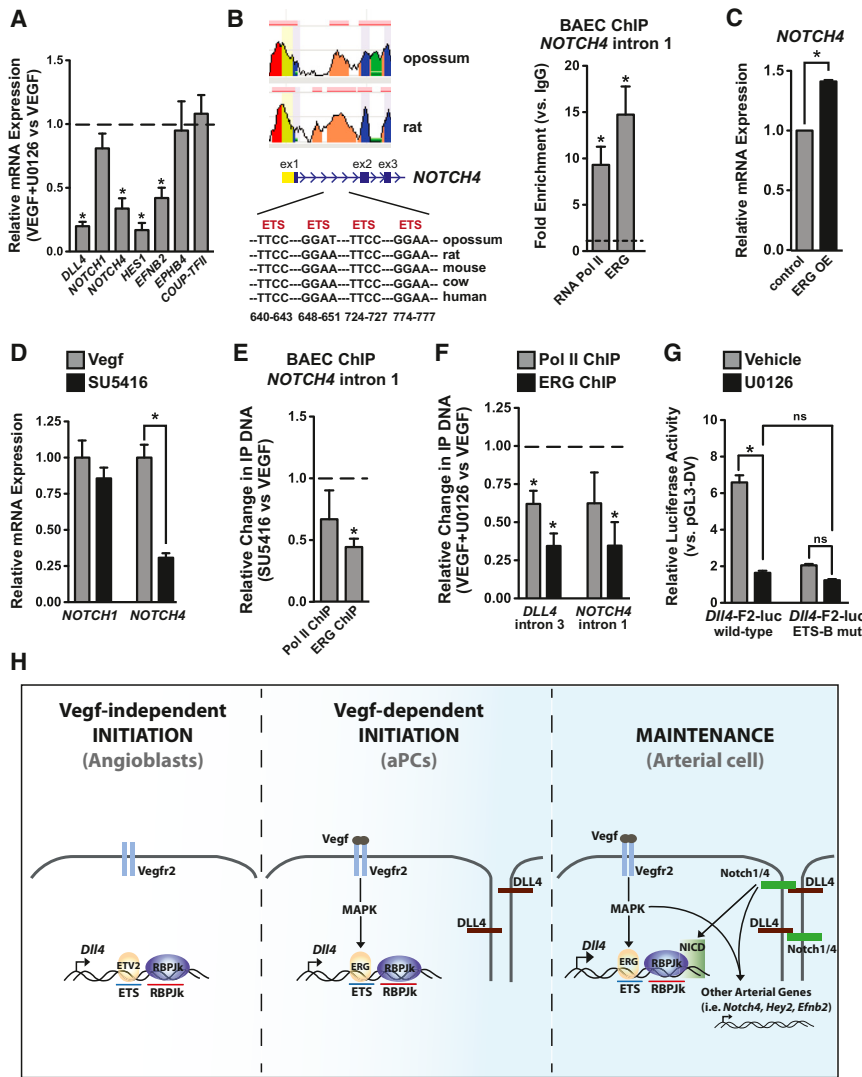


**Figure 7. Vegf/MAPK Signaling Activates Arterial Genes by Promoting ETS Factor Binding**

(A) Expression of arterial genes (*DLL4*, *NOTCH4*, *EFNB2*) and the Notch target gene, *HES1*, were decreased in VEGF-treated BAEC cotreated with the MAPK inhibitor, U0126 (n = 4). *NOTCH1* and vein markers were unaffected.

(B) An ECR (human reference genome) present in intron 1 of *NOTCH4* contains multiple conserved ETS elements and binds ERG, as assessed by ChIP assay (n = 6).

(C) Overexpression of ERG in HUVEC increased *NOTCH4* expression by qRT-PCR (n = 4).

(D) Inhibition of Vegf signaling decreased *NOTCH4* expression, but had no effect on *NOTCH1* (n = 3).

(E) Inhibition of Vegf signaling decreased ERG binding to intron 1 of *NOTCH4* (n = 5).

(F) Inhibition of MAPK signaling decreased ERG binding to *DLL4* intron 3 and *NOTCH1* intron 1 (n = 3).

(G) Inhibition of MAPK decreased F2:luciferase activity and mutation of the ETS-B site similarly decreased activity and abrogated MAPK-responsiveness. Shown is a representative experiment, triplicate determinations.

(H) Model of *Dll4* regulation during artery development. At early stages of vasculogenesis (left), ETV2 is expressed independent of Vegf signaling in angioblasts and activates the *Dll4* enhancer. At later stages of development, activity of other ETS factors, such as ERG are induced downstream of Vegf/MAPK signaling in the arterial precursor cells (aPCs) (middle), and expression of *Dll4* and *Notch4* is activated. Once *Dll4* and Notch receptors are both expressed, continued Notch signaling maintains *Dll4* enhancer activity and activates and maintains the expression of other arterial genes (right). All graphical data are mean ± SEM.

See also Figure S6.

Vegf that is required for artery specification (Coults et al., 2010). Similarly, although prior studies suggested that canonical Wnt/ $\beta$ -catenin signaling is active in early arteries (i.e., E9.5) and  $\beta$ -catenin drives *Dll4* promoter activity (Corada et al., 2010), we find no evidence of active canonical Wnt/ $\beta$ -catenin signaling in early arteries (i.e., E8.5 and E9.5) and *Dll4* expression in the dorsal aorta is intact when *Ctnnb1* is deleted from the endothelium, suggesting that  $\beta$ -catenin is dispensable for early artery specification. Finally, the genomic fragment that is located just upstream of *Dll4*—where  $\beta$ -catenin/TCF/LEF and *Foxc1/2* have been suggested to function—does not direct arterial-specific expression.

Vegf-mediated activation of Notch signaling, via NICD/RBPJK transcriptional activity is necessary and sufficient to induce downstream transcription factors, such as *Hey2* and other arterial markers, such as *Efnb2* (Swift and Weinstein, 2009). However, we postulate that Notch signaling is not required for the initiation of *Dll4* expression and primitive dorsal aortae formation. *Dll4* is the first Notch ligand expressed in the forming arteries in the mouse, and *Dll4* expression (first detected at E8.0) precedes

that of the genes encoding arterial Notch receptors, *Notch1* and *Notch4* (detected at E8.25) (Chong et al., 2011); calling into question how endothelial cell-autonomous Notch signaling could initiate *Dll4* expression. Indeed, *Notch1*<sup>-/-</sup>; *Notch4*<sup>-/-</sup> mice have normal levels of *Dll4* at E9.5 (albeit in an abnormal expression pattern), and the dorsal aortae are still formed (Krebs et al., 2000). Similarly, dorsal aortae are present when *Rbpjk* is deleted specifically in the endothelium (Krebs et al., 2004). Although the arterial enhancer of *Dll4* that we isolated (F2) contains a conserved functional binding site for RBPJK, we provide several lines of evidence demonstrating that Notch signaling is not required for the initial arterial expression of *Dll4*. First, mutation of the RBPJK site in the context of the full-length enhancer does not affect its arterial-specificity in mice or zebrafish embryos. Second, global loss of *Rbpjk* in embryonic mice or zebrafish fails to abolish enhancer activity early in arterial development. Third, early arterial expression of endogenous *Dll4* mRNA is present, albeit at reduced levels, in *Rbpjk*<sup>-/-</sup> embryos. However, endothelial-specific ablation of Notch signaling does not diminish F2 activity at E8.5 or E9.5, suggesting a possible

nonendothelial role for Notch signaling in regulating *Dll4*. Interestingly, *Dll4* enhancer activity in the dorsal aorta is greatly reduced in later-stage *rbpj* morphant zebrafish embryos, suggesting that Notch signaling maintains *Dll4* expression. Collectively, our findings demonstrate that initiation of *Dll4* expression during artery specification is Notch-independent. We propose that *Dll4* expression is initiated during vasculogenesis (through Notch-independent mechanisms; see below), and that Notch signaling subsequently becomes activated by a Vegf/MAPK/ETS pathway that regulates both *Dll4* and *Notch4* (Figure 7H). Subsequently, *Dll4* expression is maintained through a Notch-dependent positive feedback loop to sustain artery specification, as has been previously suggested (Caolo et al., 2010).

A highly conserved ETS site (i.e., ETS-B) is responsible for the majority of the activity of the arterial enhancer of *Dll4*, including its responsiveness to Vegf/MAPK signaling. How then do ETS factors, many of which are uniformly expressed in the vasculature, regulate the arterial specificity of *Dll4*? The *Dll4* enhancer can be bound (Figure S3D) and activated (data not shown) by the angioblast-enriched ETS family member ETV2 (Lee et al., 2008). Interestingly, the first angioblasts to arise during murine development appear to be arterial (Chong et al., 2011). We therefore posit that ETV2 initiates *Dll4* expression during vasculogenesis (Figure 7H). Our data further suggests that a second wave of Vegf-dependent ETS factors appears to reinforce *Dll4* expression in the forming dorsal aorta (Figure 7H). We find that Vegf regulates the expression of several zebrafish ETS factors in the endothelium, including *elf2a*, *elf2b*, *elk4*, *erg*, *ets1*, and *fli1a*. Furthermore, ERG appears to be enriched in arterial cells, implying that some ETS factors may be arterial-enriched. More importantly, we discover that the recruitment of ERG to the *Dll4* F2 enhancer and an ECR within *Notch4* is induced by Vegf/MAPK signaling. In this case, differential ERG occupancy is not mediated by changes in total ERG levels or subcellular localization, suggesting that Vegf/MAPK signaling enhances the DNA binding activity of ERG. We have also observed Vegf-dependent recruitment of ETS1 to these same enhancers (unpublished results mined from data in Zhang et al., 2013), suggesting that additional ETS family members may be regulated similarly to ERG, and cooperatively control arterial specification. Importantly, the enhanced activation of the *Dll4* enhancer and endogenous *dll4* in response to *vegfa* overexpression can be attenuated by knockdown of *erg* and *fli1a*, suggesting that ETS factors are necessary for the Vegf-induced expression of *Dll4*. We also find reduced *Dll4* expression in the dorsal aorta of *Erg*<sup>ΔEx4/ΔEx4</sup> mice and in *erg/fli1a* morphant zebrafish embryos, but failed to observe AVMs, suggesting that other ETS factors compensate in the specification of the early artery.

Vegf is known to selectively activate MAPK signaling in arteries compared to veins during embryogenesis (Corson et al., 2003; Hong et al., 2006). Interestingly, several ETS family members are phosphorylated by MAPKs (Hill et al., 1993; Murakami et al., 2011; Petrovic et al., 2003), and these modifications are known to affect their interaction with other transcription factors as well as their binding to DNA (Hollenhorst et al., 2011). Future experiments will examine ETS factor phosphorylation downstream of Vegf/MAPK signaling and whether ETS factors functionally interact with other transcription factor families to establish arterial fate. Finally, we also demonstrate that a Vegf/

MAPK/ETS pathway regulates *Notch4*, suggesting that this pathway lies upstream of induction of Notch signaling in the arterial endothelium. Indeed, we observe reduced Notch-regulated gene expression and Notch-dependent reporter activity in embryos with reduced ETS activity. Interestingly, *Notch4* is not as sensitive as *Dll4* to ERG overexpression (Figure 4B versus Figure 7C), which may in part explain the delay in *Notch4* expression during artery formation (Chong et al., 2011).

In summary, we have uncovered a genetic pathway that integrates Vegf signaling, ETS-dependent transcriptional regulation, and the induction of one of the earliest, essential ligands for artery specification and Notch pathway activation, *Dll4*. This same pathway also regulates the expression of *Notch4*, an arterial-specific receptor for *Dll4*, and appears to initiate Notch signaling in the artery. These findings may provide insight into congenital defects in AV specification and maintenance and suggest approaches to direct endothelial cells toward the arterial lineage.

## EXPERIMENTAL PROCEDURES

### Bioinformatic Analyses, Cloning, Mutagenesis, Generation of Transgenic Mice, and Mouse Lines Used

See Supplemental Experimental Procedures for details.

### Mouse Experiments

All mouse protocols were approved by the Institutional Animal Care and Use Committee at UCSF and Harvard Medical School. Histology and in situ hybridization (Dodou et al., 2003; Wythe et al., 2011), ink injections (Krebs et al., 2004), and CD31 immunofluorescence (Coults et al., 2010) were performed as described elsewhere.

### Electrophoretic Mobility Shift Assay

DNA binding assays were performed as described previously (Dodou et al., 2003). See Supplemental Experimental Procedures for details.

### Cell Culture, Immunofluorescence, Luciferase Analysis, and ChIP

Human umbilical vein endothelial cells (HUVECs) (ScienCell) and Bovine arterial endothelial cells (BAECs) (Lonza) were grown in endothelial media (ScienCell). BAECs were treated with 50 ng/ml recombinant Vegf-A<sub>165</sub> (R&D Systems), 0.5 μM SU5416 (Sigma), 20 μM U0126 (Invivogen), or 10 μM LY29004 (Cell Signaling) for 24 hr. Immunofluorescence of ERG and phalloidin was performed as described (Finn et al., 2011) using ERG antibody (Santa Cruz, C-20, 1:100 dilution). pCS2-6xMYC-Etv2 (De Val et al., 2008) has been described and pCMV-Sport6-ERG was from Open Biosystems (IMAGE clone 6052140). Cloning of pCS2-V5-ERG is described in Supplemental Experimental Procedures. Luciferase experiments were performed as described (Cheng et al., 2013). Electroporation of HUVEC was performed using a Lonza 4D Nucleofector with the P5 Primary Cell Kit with 2.5 μg of expression construct and 0.5 μg of pmaxGFP. ChIP was performed using the Imprint Kit (Sigma) with 1 μg of antibody: RNA Pol II (mouse monoclonal, Sigma), ERG (rabbit polyclonal, Santa Cruz, C-20), V5 (mouse monoclonal, Invitrogen), or NICD (rabbit polyclonal, ChIP grade, Abcam). IgG (mouse, Sigma) was used as a negative control. Fold enrichment was calculated by determining the fold change of qPCR values for the specific antibody compared to IgG control. See Supplemental Experimental Procedures for primer sequences.

### Zebrafish Experiments

Zebrafish protocols were approved by the Animal Care Committee at the University Health Network and UCSF. The following transgenic lines were utilized: *Tg(kdrl:ras-mCherry)*<sup>s896</sup> (Chi et al., 2008), *Tg(kdrl:GFP)*<sup>s843</sup> (Jin et al., 2005), and *Tg(EPV.Tp1-MmuHbb:EGFP)*<sup>um14</sup> (Parsons et al., 2009). See Supplemental Experimental Procedures for generation of *Tg(Dll4-F2-E1b:GFP)* and experimental details.

**qRT-PCR**

qRT-PCR was performed as before (Fish et al., 2008). See [Supplemental Experimental Procedures](#) for details and primer sequences.

**Western Blot**

Western blotting was performed as described previously (Fish et al., 2011) using ERG (rabbit polyclonal, Santa Cruz, C-20), Sin3a (Santa Cruz, AK-11), V5 (mouse monoclonal, Invitrogen), or GAPDH (mouse monoclonal, Santa Cruz) (mouse monoclonal, Abcam) antibodies. Cells were starved overnight and treated with 50 ng/ml recombinant Vegf-A<sub>165</sub> (R&D Systems) for 20 min before harvesting for subcellular fractionation, as previously described (Wythe et al., 2011). HUVEC and HUAEC lysates were purchased from ScienCell.

**Statistics**

All graphs depict the mean  $\pm$  SEM of at least three independent experiments unless otherwise indicated. Statistical significance was performed using a Student's t test, ANOVA, or  $\chi^2$  test as appropriate.

**SUPPLEMENTAL INFORMATION**

Supplemental Information includes Supplemental Experimental Procedures and six figures and can be found with this article online at <http://dx.doi.org/10.1016/j.devcel.2013.06.007>.

**ACKNOWLEDGMENTS**

The authors thank Hilary Clay for zebrafish core facility guidance and Dario Miguel-Perez and Claire Cutting for mouse care and husbandry. J.D.W. was supported by a Scientist Development Grant from the American Heart Association (12SDG12060353) and National Institutes of Health (NIH) (5T32-HL007544). W.P.D. was supported by the California Institute of Regenerative Medicine (TG2-01160) and NIH (5T32-HL007731-20). S.T.A. is an American Australian Association Morgan Stanley Pediatrics Fellow, and S.T.A. and P.O. were supported by the NIH (PO1 HL76540). D.Y.R.S. was supported by the NIH (HL54737) and the Packard Foundation. This work was supported by grants from the NHLBI (PO1 HL089707 to B.G.B and B.L.B. and HL64658 to B.L.B.), an operating grant from the Canadian Institutes of Health Research (MOP-119506 to J.E.F.), an Early Researcher Award (Ontario Ministry of Economic Development and Innovation, to J.E.F.), a Leaders Opportunity Fund Award (Canada Foundation for Innovation, to J.E.F.), and a New Investigator Award (Heart and Stroke Foundation of Canada, to J.E.F.). B.L.B. is supported by an Innovative Science Award (12PILT12670005) from the American Heart Association, Western States Affiliate. B.G.B. holds the Lawrence J. and Florence A. DeGeorge Charitable Trust/American Heart Association Established Investigator Award. This work was also supported by an NIH/NCRR grant (C06 RR018928) to the J. David Gladstone Institutes and by William H. Younger, Jr. (to B.G.B.).

Received: February 6, 2013

Revised: May 28, 2013

Accepted: June 7, 2013

Published: July 3, 2013

**REFERENCES**

- Bi, W., Drake, C.J., and Schwarz, J.J. (1999). The transcription factor MEF2C-null mouse exhibits complex vascular malformations and reduced cardiac expression of angiotensin I and VEGF. *Dev. Biol.* *211*, 255–267.
- Caolo, V., van den Akker, N.M., Verbruggen, S., Donners, M.M., Swennen, G., Schulten, H., Waltenberger, J., Post, M.J., and Molin, D.G. (2010). Feed-forward signaling by membrane-bound ligand receptor circuit: the case of NOTCH DELTA-like 4 ligand in endothelial cells. *J. Biol. Chem.* *285*, 40681–40689.
- Cattelino, A., Liebner, S., Gallini, R., Zanetti, A., Balconi, G., Corsi, A., Bianco, P., Wolburg, H., Moore, R., Oreda, B., et al. (2003). The conditional inactivation of the beta-catenin gene in endothelial cells causes a defective vascular pattern and increased vascular fragility. *J. Cell Biol.* *162*, 1111–1122.
- Cheng, H.S., Sivachandran, N., Lau, A., Boudreau, E., Zhao, J.L., Baltimore, D., Delgado-Olguin, P., Cybulsky, M.I., and Fish, J.E. (2013). MicroRNA-146 represses endothelial activation by inhibiting pro-inflammatory pathways. *EMBO Mol. Med.*, in press. Published online June 3, 2013. <http://dx.doi.org/10.1002/emmm.201202318>.
- Chi, N.C., Shaw, R.M., De Val, S., Kang, G., Jan, L.Y., Black, B.L., and Stainier, D.Y. (2008). Foxn4 directly regulates tbx2b expression and atrioventricular canal formation. *Genes Dev.* *22*, 734–739.
- Chong, D.C., Koo, Y., Xu, K., Fu, S., and Cleaver, O. (2011). Stepwise arteriovenous fate acquisition during mammalian vasculogenesis. *Dev. Dyn.* *240*, 2153–2165.
- Corada, M., Nyqvist, D., Orsenigo, F., Caprini, A., Giampietro, C., Taketo, M.M., Iruela-Arispe, M.L., Adams, R.H., and Dejana, E. (2010). The Wnt/beta-catenin pathway modulates vascular remodeling and specification by upregulating Dll4/Notch signaling. *Dev. Cell* *18*, 938–949.
- Corson, L.B., Yamanaka, Y., Lai, K.M., and Rossant, J. (2003). Spatial and temporal patterns of ERK signaling during mouse embryogenesis. *Development* *130*, 4527–4537.
- Coultas, L., Nieuwenhuis, E., Anderson, G.A., Cabezas, J., Nagy, A., Henkelman, R.M., Hui, C.C., and Rossant, J. (2010). Hedgehog regulates distinct vascular patterning events through VEGF-dependent and -independent mechanisms. *Blood* *116*, 653–660.
- De Val, S., and Black, B.L. (2009). Transcriptional control of endothelial cell development. *Dev. Cell* *16*, 180–195.
- De Val, S., Chi, N.C., Meadows, S.M., Minovitsky, S., Anderson, J.P., Harris, I.S., Ehlers, M.L., Agarwal, P., Visel, A., Xu, S.M., et al. (2008). Combinatorial regulation of endothelial gene expression by ets and forkhead transcription factors. *Cell* *135*, 1053–1064.
- Deng, Y., Larrivée, B., Zhuang, Z.W., Atri, D., Moraes, F., Praht, C., Eichmann, A., and Simons, M. (2013). Endothelial RAF1/ERK activation regulates arterial morphogenesis. *Blood* *121*, 3988–3996.
- Dodou, E., Xu, S.M., and Black, B.L. (2003). mef2c is activated directly by myogenic basic helix-loop-helix proteins during skeletal muscle development in vivo. *Mech. Dev.* *120*, 1021–1032.
- Duarte, A., Hirashima, M., Benedito, R., Trindade, A., Diniz, P., Bekman, E., Costa, L., Henrique, D., and Rossant, J. (2004). Dosage-sensitive requirement for mouse Dll4 in artery development. *Genes Dev.* *18*, 2474–2478.
- Fish, J.E., Santoro, M.M., Morton, S.U., Yu, S., Yeh, R.F., Wythe, J.D., Ivey, K.N., Bruneau, B.G., Stainier, D.Y., and Srivastava, D. (2008). miR-126 regulates angiogenic signaling and vascular integrity. *Dev. Cell* *15*, 272–284.
- Fish, J.E., Wythe, J.D., Xiao, T., Bruneau, B.G., Stainier, D.Y., Srivastava, D., and Woo, S. (2011). A Slit/miR-218/Robo regulatory loop is required during heart tube formation in zebrafish. *Development* *138*, 1409–1419.
- Gale, N.W., Dominguez, M.G., Noguera, I., Pan, L., Hughes, V., Valenzuela, D.M., Murphy, A.J., Adams, N.C., Lin, H.C., Holash, J., et al. (2004). Haploinsufficiency of delta-like 4 ligand results in embryonic lethality due to major defects in arterial and vascular development. *Proc. Natl. Acad. Sci. USA* *101*, 15949–15954.
- Ghosh, S., Basu, M., and Roy, S.S. (2012). ETS-1 protein regulates vascular endothelial growth factor-induced matrix metalloproteinase-9 and matrix metalloproteinase-13 expression in human ovarian carcinoma cell line SKOV-3. *J. Biol. Chem.* *287*, 15001–15015.
- Heo, S.H., Choi, Y.J., Ryoo, H.M., and Cho, J.Y. (2010). Expression profiling of ETS and MMP factors in VEGF-activated endothelial cells: role of MMP-10 in VEGF-induced angiogenesis. *J. Cell. Physiol.* *224*, 734–742.
- Hill, C.S., Marais, R., John, S., Wynne, J., Dalton, S., and Treisman, R. (1993). Functional analysis of a growth factor-responsive transcription factor complex. *Cell* *73*, 395–406.
- Hollenhorst, P.C., McIntosh, L.P., and Graves, B.J. (2011). Genomic and biochemical insights into the specificity of ETS transcription factors. *Annu. Rev. Biochem.* *80*, 437–471.
- Hong, C.C., Peterson, Q.P., Hong, J.Y., and Peterson, R.T. (2006). Artery/vein specification is governed by opposing phosphatidylinositol-3 kinase and MAP kinase/ERK signaling. *Curr. Biol.* *16*, 1366–1372.



- Jin, S.W., Beis, D., Mitchell, T., Chen, J.N., and Stainier, D.Y. (2005). Cellular and molecular analyses of vascular tube and lumen formation in zebrafish. *Development* *132*, 5199–5209.
- Krebs, L.T., Xue, Y., Norton, C.R., Shutter, J.R., Maguire, M., Sundberg, J.P., Gallahan, D., Closson, V., Kitajewski, J., Callahan, R., et al. (2000). Notch signaling is essential for vascular morphogenesis in mice. *Genes Dev.* *14*, 1343–1352.
- Krebs, L.T., Shutter, J.R., Tanigaki, K., Honjo, T., Stark, K.L., and Gridley, T. (2004). Haploinsufficient lethality and formation of arteriovenous malformations in Notch pathway mutants. *Genes Dev.* *18*, 2469–2473.
- Krebs, L.T., Starling, C., Chervonsky, A.V., and Gridley, T. (2010). Notch1 activation in mice causes arteriovenous malformations phenocopied by ephrinB2 and EphB4 mutants. *Genesis* *48*, 146–150.
- Lawson, N.D., Scheer, N., Pham, V.N., Kim, C.H., Chitnis, A.B., Campos-Ortega, J.A., and Weinstein, B.M. (2001). Notch signaling is required for arterial-venous differentiation during embryonic vascular development. *Development* *128*, 3675–3683.
- Lawson, N.D., Vogel, A.M., and Weinstein, B.M. (2002). *sonic hedgehog* and *vascular endothelial growth factor* act upstream of the Notch pathway during arterial endothelial differentiation. *Dev. Cell* *3*, 127–136.
- Lee, D., Park, C., Lee, H., Lugas, J.J., Kim, S.H., Arentson, E., Chung, Y.S., Gomez, G., Kyba, M., Lin, S., et al. (2008). ER71 acts downstream of BMP, Notch, and Wnt signaling in blood and vessel progenitor specification. *Cell Stem Cell* *2*, 497–507.
- Lin, Q., Lu, J., Yanagisawa, H., Webb, R., Lyons, G.E., Richardson, J.A., and Olson, E.N. (1998). Requirement of the MADS-box transcription factor MEF2C for vascular development. *Development* *125*, 4565–4574.
- Liu, F., and Patient, R. (2008). Genome-wide analysis of the zebrafish ETS family identifies three genes required for hemangioblast differentiation or angiogenesis. *Circ. Res.* *103*, 1147–1154.
- Liu, Z.J., Shirakawa, T., Li, Y., Soma, A., Oka, M., Dotto, G.P., Fairman, R.M., Velazquez, O.C., and Herlyn, M. (2003). Regulation of Notch1 and Dll4 by vascular endothelial growth factor in arterial endothelial cells: implications for modulating arteriogenesis and angiogenesis. *Mol. Cell. Biol.* *23*, 14–25.
- Luo, H., Jin, K., Xie, Z., Qiu, F., Li, S., Zou, M., Cai, L., Hozumi, K., Shima, D.T., and Xiang, M. (2012). Forkhead box N4 (Foxn4) activates Dll4-Notch signaling to suppress photoreceptor cell fates of early retinal progenitors. *Proc. Natl. Acad. Sci. USA* *109*, E553–E562.
- Marchuk, D.A. (1998). Genetic abnormalities in hereditary hemorrhagic telangiectasia. *Curr. Opin. Hematol.* *5*, 332–338.
- Murakami, M., Nguyen, L.T., Hatanaka, K., Schachterle, W., Chen, P.Y., Zhuang, Z.W., Black, B.L., and Simons, M. (2011). FGF-dependent regulation of VEGF receptor 2 expression in mice. *J. Clin. Invest.* *121*, 2668–2678.
- Oka, C., Nakano, T., Wakeham, A., de la Pompa, J.L., Mori, C., Sakai, T., Okazaki, S., Kawaichi, M., Shiota, K., Mak, T.W., and Honjo, T. (1995). Disruption of the mouse RBP-J kappa gene results in early embryonic death. *Development* *121*, 3291–3301.
- Parsons, M.J., Pisharath, H., Yusuff, S., Moore, J.C., Siekmann, A.F., Lawson, N., and Leach, S.D. (2009). Notch-responsive cells initiate the secondary transition in larval zebrafish pancreas. *Mech. Dev.* *126*, 898–912.
- Petrovic, N., Bhagwat, S.V., Ratzan, W.J., Ostrowski, M.C., and Shapiro, L.H. (2003). CD13/APN transcription is induced by RAS/MAPK-mediated phosphorylation of Ets-2 in activated endothelial cells. *J. Biol. Chem.* *278*, 49358–49368.
- Ren, B., Deng, Y., Mukhopadhyay, A., Lanahan, A.A., Zhuang, Z.W., Moodie, K.L., Mulligan-Kehoe, M.J., Byzova, T.V., Peterson, R.T., and Simons, M. (2010). ERK1/2-Akt1 crosstalk regulates arteriogenesis in mice and zebrafish. *J. Clin. Invest.* *120*, 1217–1228.
- Seo, S., Fujita, H., Nakano, A., Kang, M., Duarte, A., and Kume, T. (2006). The forkhead transcription factors, Foxc1 and Foxc2, are required for arterial specification and lymphatic sprouting during vascular development. *Dev. Biol.* *294*, 458–470.
- Shalaby, F., Rossant, J., Yamaguchi, T.P., Gertsenstein, M., Wu, X.F., Breitman, M.L., and Schuh, A.C. (1995). Failure of blood-island formation and vasculogenesis in Flk-1-deficient mice. *Nature* *376*, 62–66.
- Swift, M.R., and Weinstein, B.M. (2009). Arterial-venous specification during development. *Circ. Res.* *104*, 576–588.
- Vijayaraj, P., Le Bras, A., Mitchell, N., Kondo, M., Juliao, S., Wasserman, M., Beeler, D., Spokes, K., Aird, W.C., Baldwin, H.S., and Oettgen, P. (2012). Erg is a crucial regulator of endocardial-mesenchymal transformation during cardiac valve morphogenesis. *Development* *139*, 3973–3985.
- Vokes, S.A., Yatskievych, T.A., Heimark, R.L., McMahon, J., McMahon, A.P., Antin, P.B., and Krieg, P.A. (2004). Hedgehog signaling is essential for endothelial tube formation during vasculogenesis. *Development* *131*, 4371–4380.
- Wang, L., Fan, C., Topol, S.E., Topol, E.J., and Wang, Q. (2003). Mutation of MEF2A in an inherited disorder with features of coronary artery disease. *Science* *302*, 1578–1581.
- Wythe, J.D., Jurynek, M.J., Urness, L.D., Jones, C.A., Sabeh, M.K., Werdich, A.A., Sato, M., Yost, H.J., Grunwald, D.J., Macrae, C.A., and Li, D.Y. (2011). Hadp1, a newly identified Pleckstrin homology domain protein, is required for cardiac contractility in zebrafish. *Dis. Model. Mech.* *4*, 607–621.
- Yamamizu, K., Matsunaga, T., Uosaki, H., Fukushima, H., Katayama, S., Hiraoka-Kanie, M., Mitani, K., and Yamashita, J.K. (2010). Convergence of Notch and beta-catenin signaling induces arterial fate in vascular progenitors. *J. Cell Biol.* *189*, 325–338.
- Zhang, B., Day, D.S., Ho, J.W., Song, L., Cao, J., Christodoulou, D., Seidman, J.G., Crawford, G.E., Park, P.J., and Pu, W.T. (2013). A dynamic H3K27ac signature identifies VEGFA-stimulated endothelial enhancers and requires EP300 activity. *Genome Res.* *23*, 917–927.

Developmental Cell, Volume 26

## Supplemental Information

### ETS Factors Regulate

### Vegf-Dependent Arterial Specification

Joshua D. Wythe, Lan T.H. Dang, W. Patrick Devine, Emilie Boudreau, Stanley T. Artap, Daniel He, William Schachterle, Didier Y.R. Stainier, Peter Oettgen, Brian L. Black, Benoit G. Bruneau, and Jason E. Fish

#### Inventory of Supplemental Information:

##### Supplemental Figures, Tables and Legends

Figure S1: This figure supplements the *Dll4* enhancer analysis of Figure 1 and demonstrates that the genomic region directly upstream of *Dll4* does not drive arterial-specific expression. It also demonstrates that Wnt/ $\beta$ -Catenin signaling is not active in early arteries and does not regulate early *Dll4* expression.

Figure S2: This figure supplements the analysis of *Dll4* enhancer *cis* elements in Figures 2 and 3 and demonstrates that MEF2C and RBPJK can bind to the F2 enhancer. This figure also demonstrates that over-expression of NICD in the endothelium can drive F2 expression in the vein, while MEF2C is dispensable for early arterial *Dll4* expression.

Figure S3: This figure supplements the functional analysis of ETS factors in *Dll4* regulation in Figure 4 and details the ETS sites present in the enhancer and their ability to bind ETS proteins.

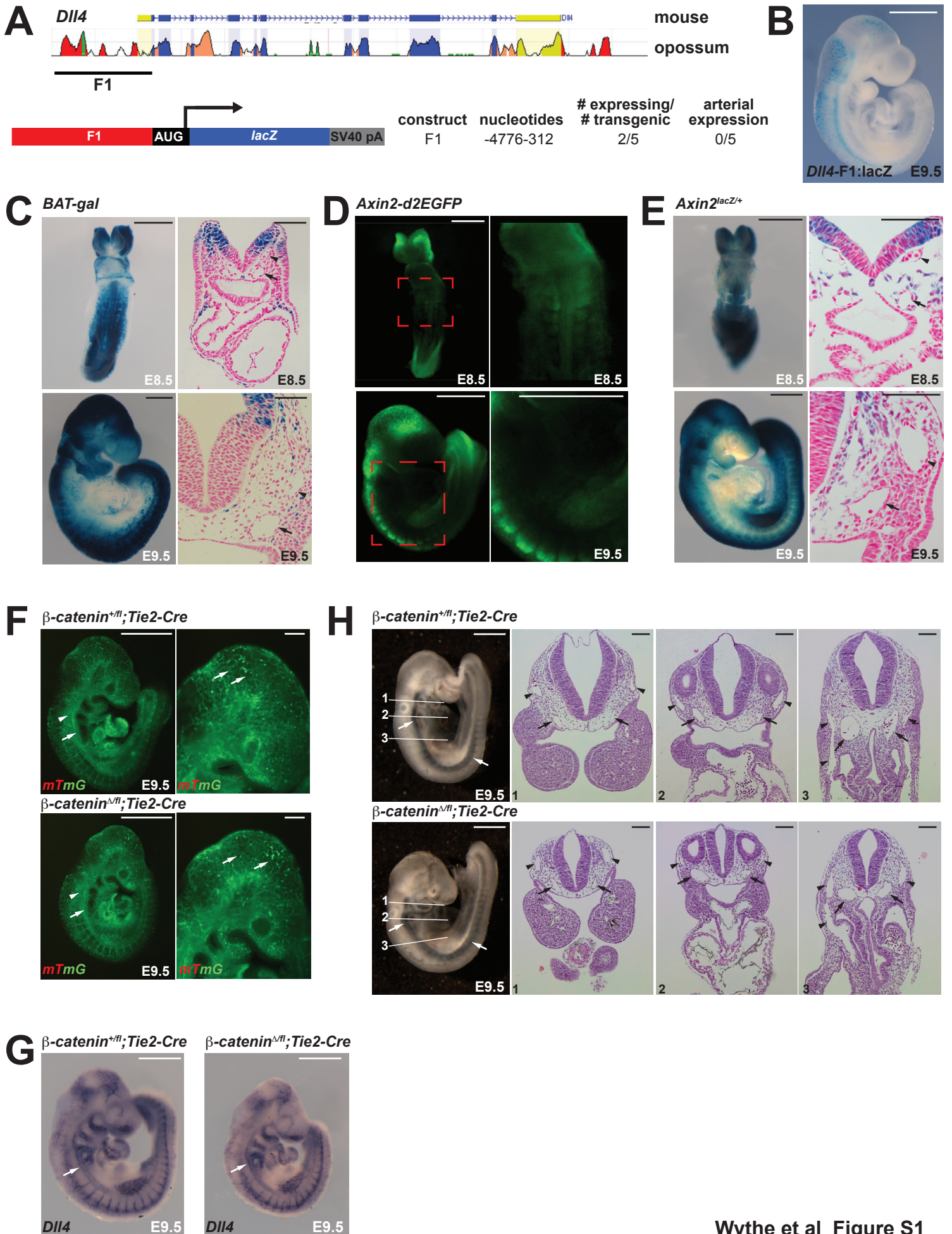
Figure S4: This figure supplements the investigation of ERG function in Figure 4 and provides detailed ERG gain- and loss-of-function phenotypes.

Figure S5: This figure supplements the analysis of Vegf regulation of ETS factors and *Dll4* in Figure 5. It shows that F2 enhancer activity is regulated by Vegf in mouse embryos and that ETS factors are regulated by Vegf at early stages of zebrafish embryogenesis.

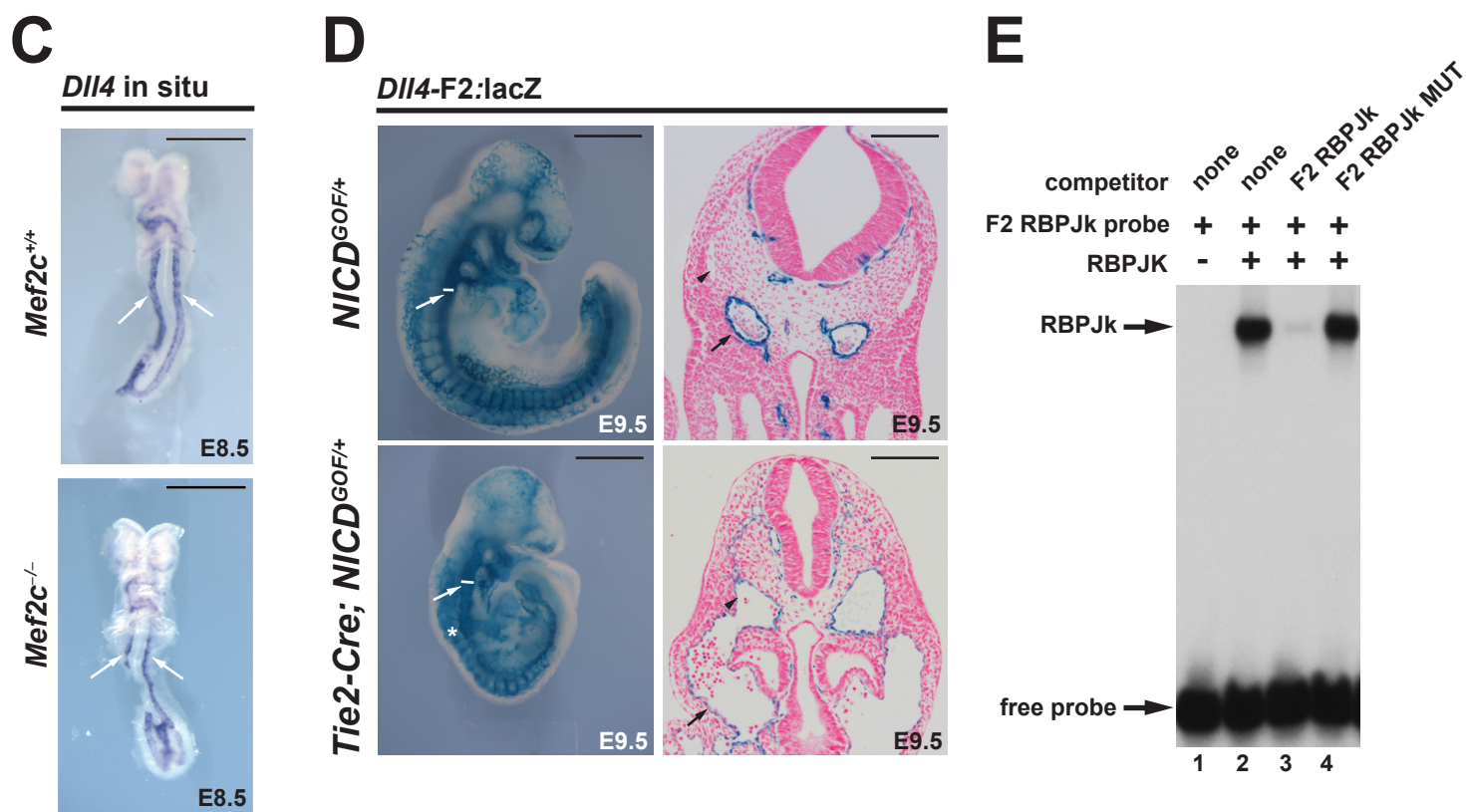
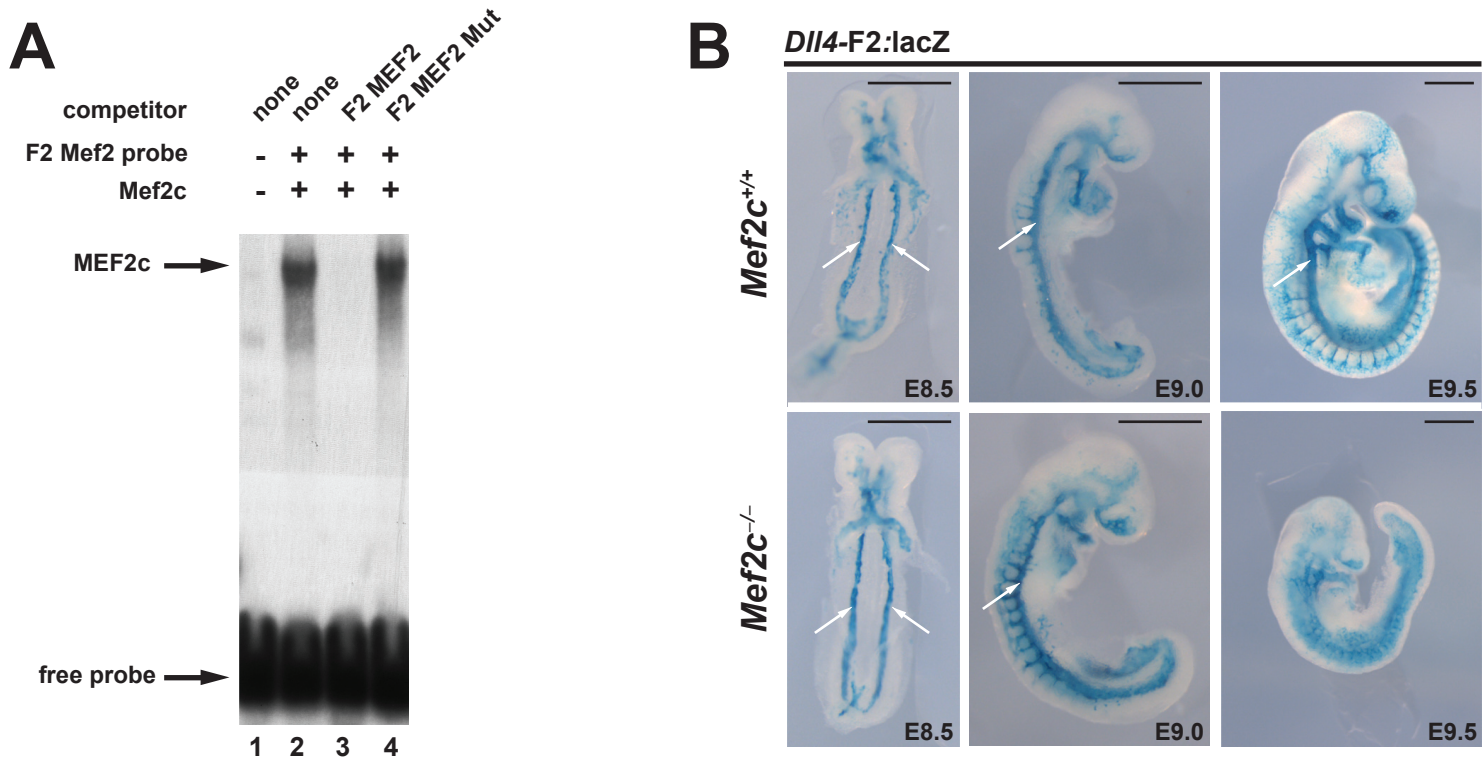
Figure S6: This figure supplements the analysis of *Dll4* regulation by Vegf/ETS in Figures 6 and 7, and demonstrates that the F2 enhancer and endogenous *Dll4* expression are regulated by Vegf/MAP kinase signaling.

##### Supplemental Experimental Procedures

##### Supplemental References

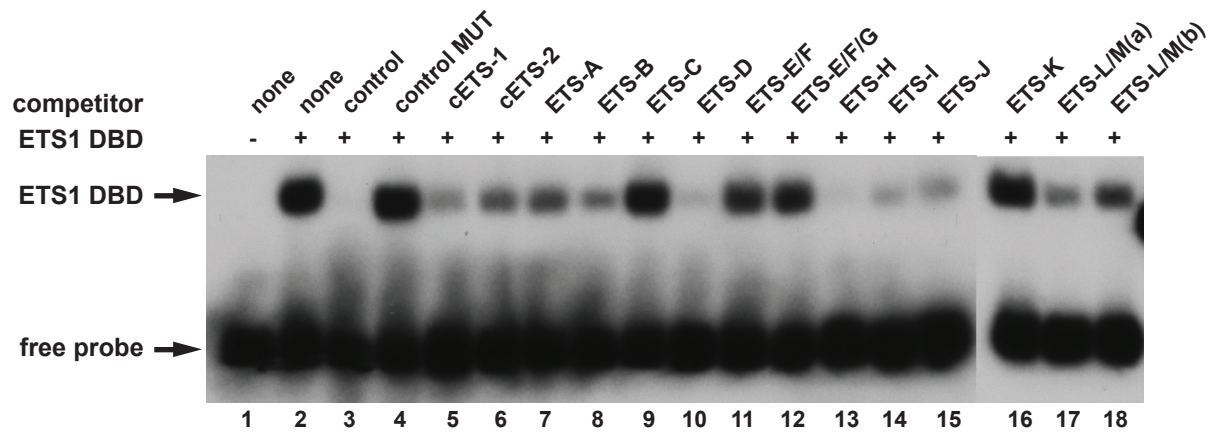
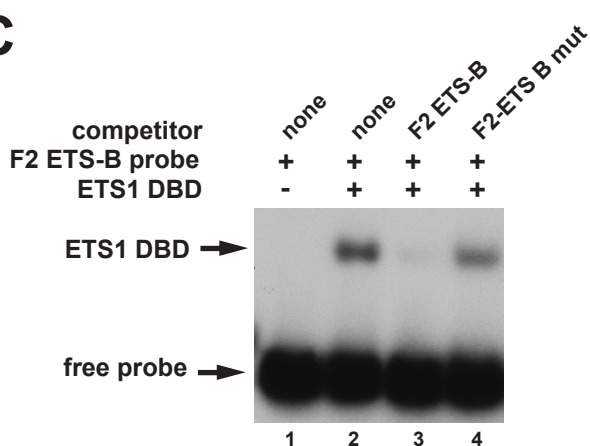
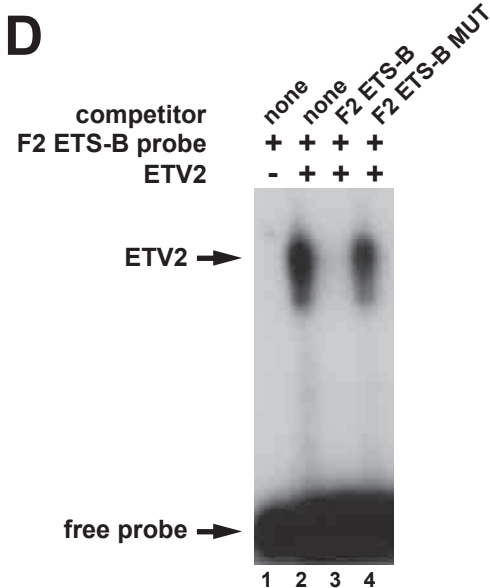




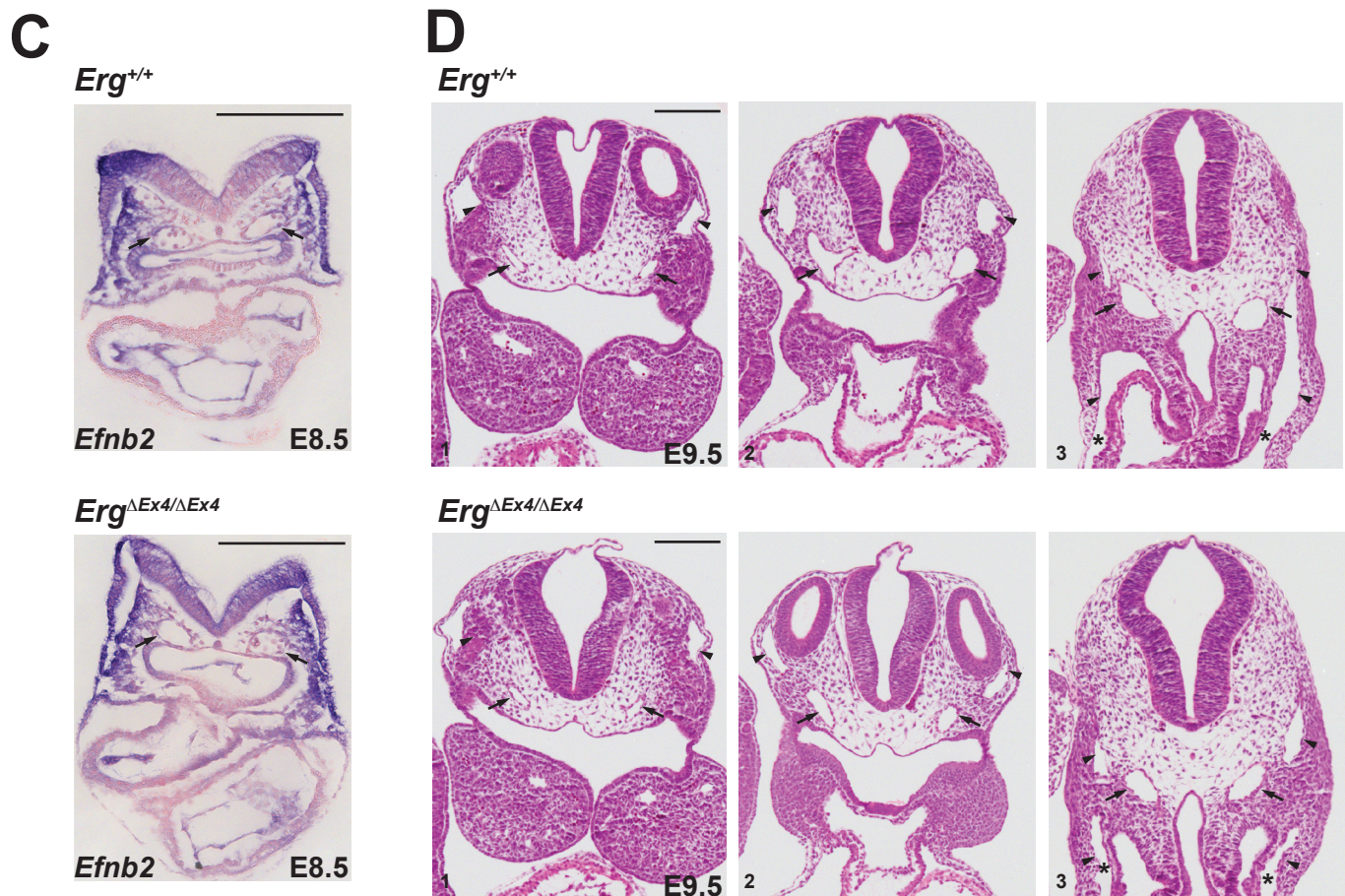
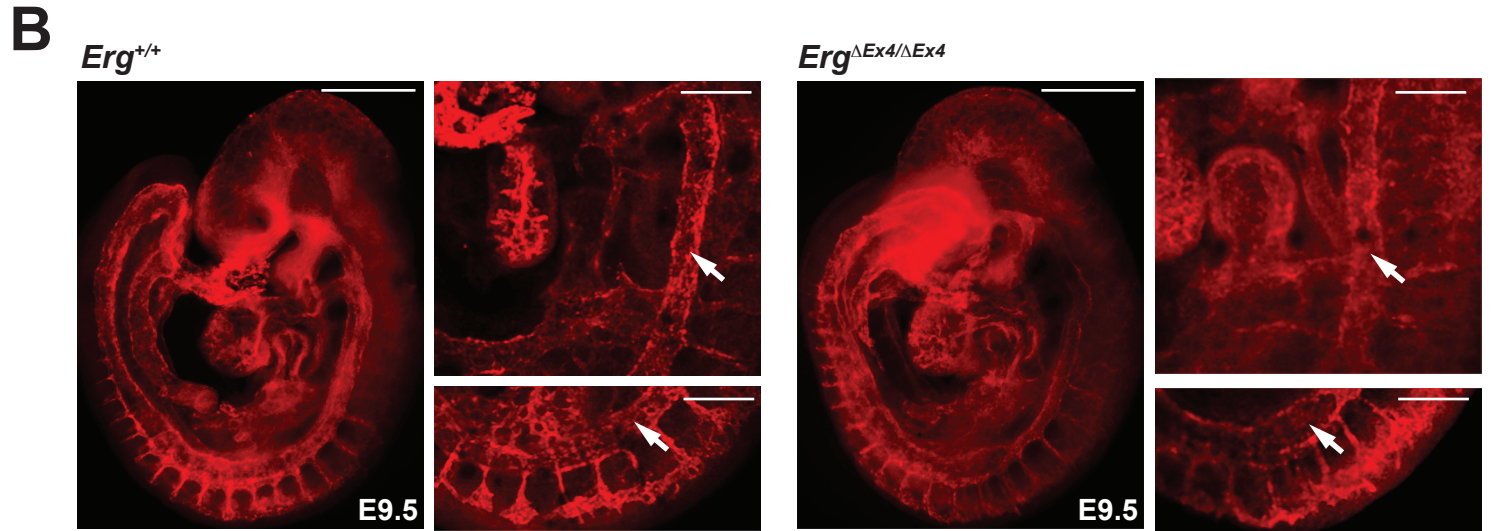
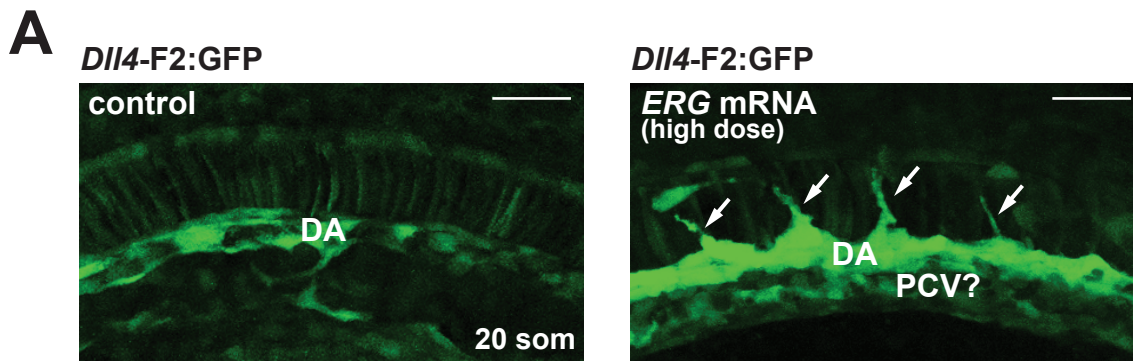


**A**

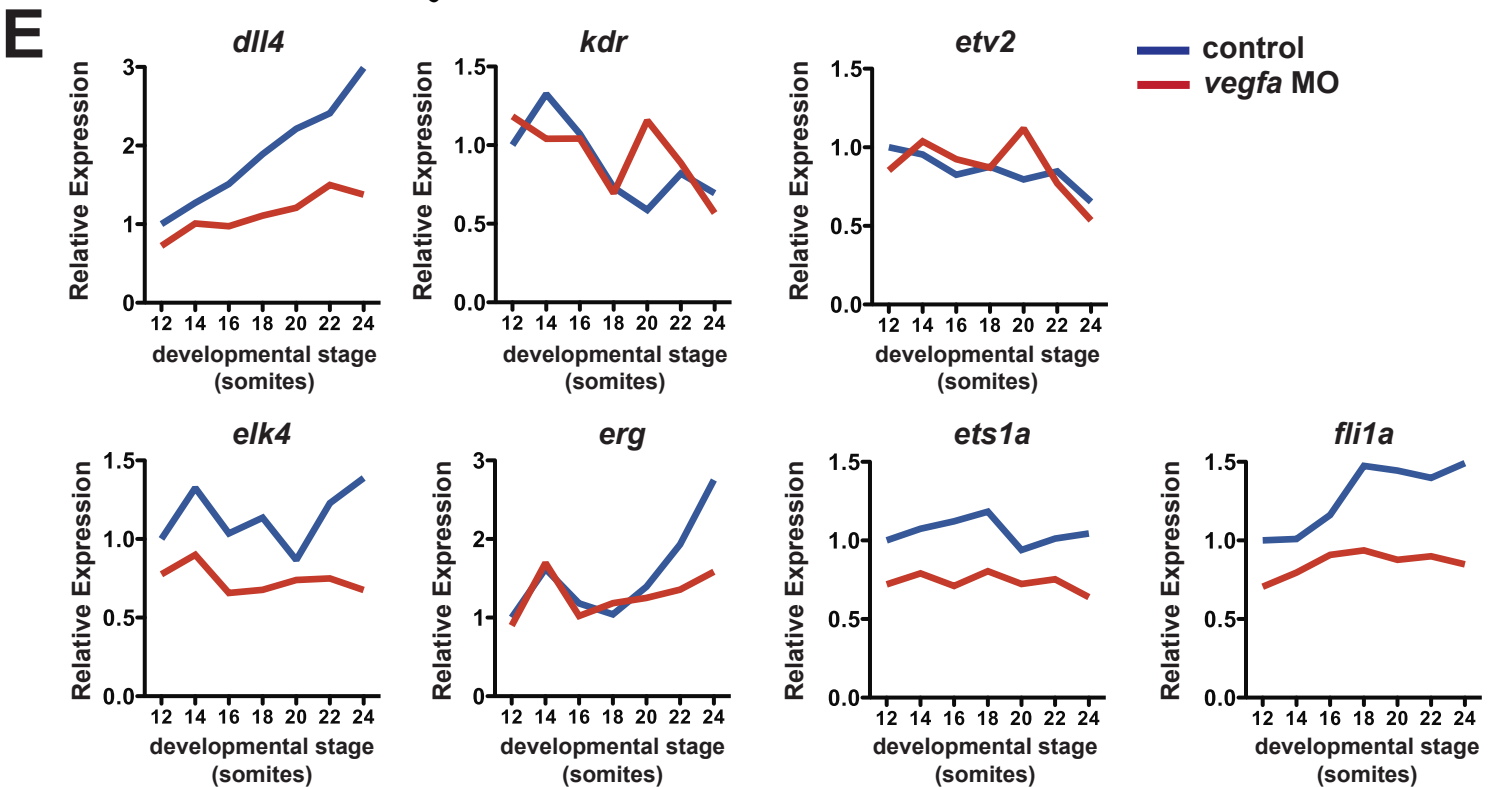
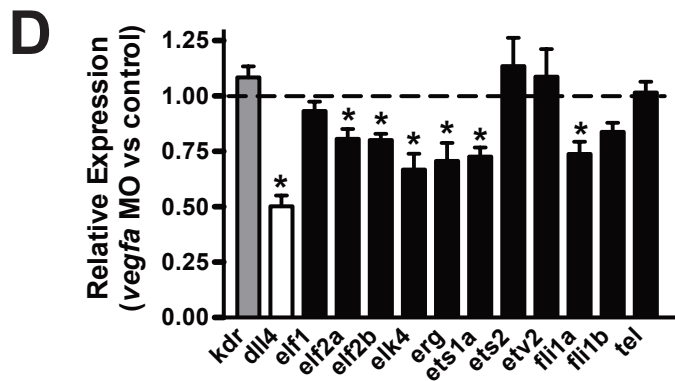
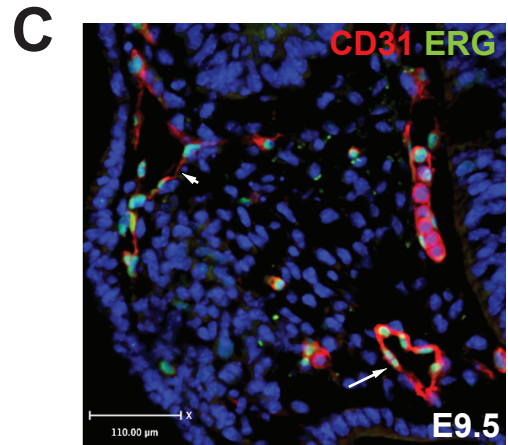
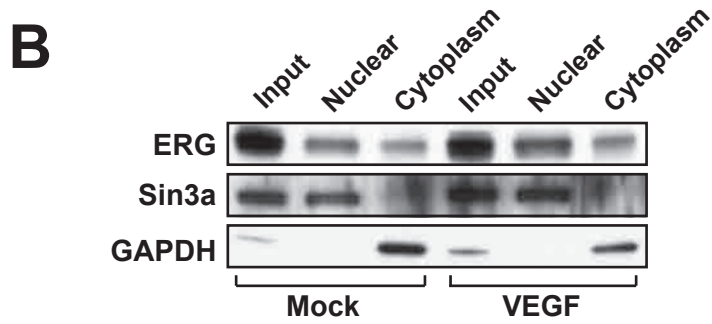
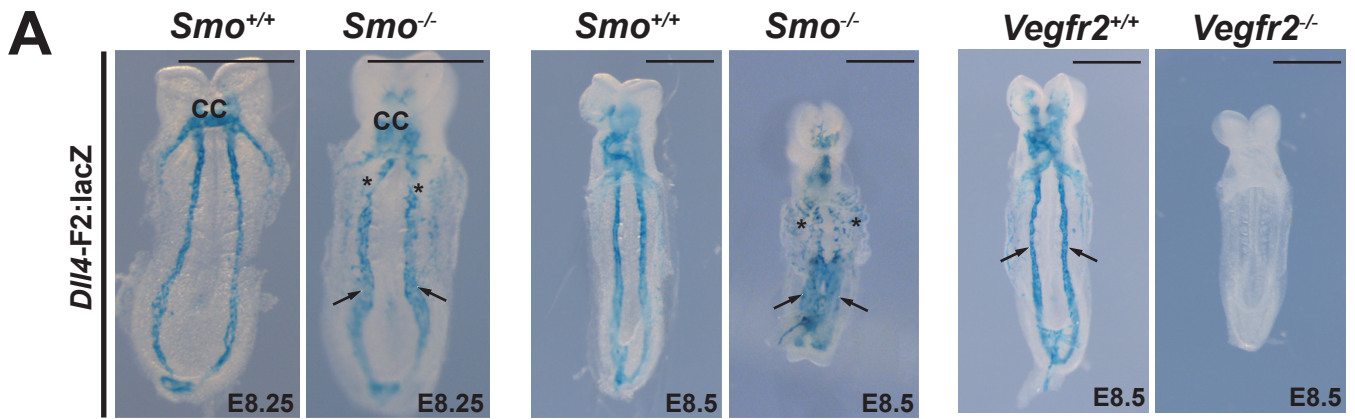
**Opossum** -----GGCCACTGGAGGGCGATAATGCTCATCATGTAGCTGGGGGCCGAAGGGTT  
**Human** ----CTCGCTCCGC CACCACAGGGGGGCGA-----CACGGCGCAGC-----GCCGAAAGAGTT  
**Mouse** GTATCTAACTTCTC GGCCACAGGGGGGCGA-----CATCACACAGC-----GCCGAAAGAGTT 56  
  
AACCTGGAAACAGGTGGGAAATAAGCGGTTGGGGAGGGTGGGGGGTGTGTTTTGGGTTTTTTTGTGGG  
AATCTGTTC-----TAGGCGGGGGAAG-----TGGGGGCTT-----  
AACCAAGTTA-----TAGGCGGGGTTGGGGGA-----CGCAGGCTT----- 101  
GGGGCAACAAGAGGGTCGTAGGTGGTGGAGCCCTGGCTAGACTGCTTCTTTGGGACTCAGTAGCTGCCG  
GGGG-----TGGGAGCAGGACGCTTAGCTTGGCCT-----GGAGCTGCCG  
GGGG-----GTGGGGCCAGGACGCTTAGCTTGGCC-----GGAGCTGCCG 142  
  
**ETS-A** **ETS-B / cETS-1**  
CCCTAGCTGGCGTCTGA **TCCGCCAGCTCCCTAATCTC-TAGCACAATTGAGTTCCTGCGGGTATTTTT**  
CCCGCGCTGGACGCTCGGAT **TCCGCTCGCTGCCTGGACTCAGAGCACAATTCGCTTCCGCGGGTATTTTT**  
CCCGCGCTGGACGCTCGGAT **TCCGCTCGCTGCCTGGACTCAGAGCACAATTCGCTTCCGCGGGTATTTTT** 215  
  
**ETS-C**  
**GGCGTGGGAAACGTGGGAGCATGGCGGTGAGAAA GGCCAGTGGTTCAGCGGCCTGACGGGCCCC**  
**GGCGTGGGAAACCGGGGAGTACGGCGGTGAGAAA GGCT-GAAGCTGCCAGCGCCCTGACGGGCCCC**  
**GGCGTGGGAAACCGGGGAGCACGGCGGTGAGAAA GGCC-GAGGCTGCCAGCGCCCTGACGGGCCCC** 282  
  
**ETS-D** **ETS-E** **ETS-F/G**  
**TCCGTATTTTACACCTTTTGCGAAATCCGCTCTTTTGGAAAGGGAAATATGGCTTTGGGATGTTGTTCTGAC**  
**TCCTGTATTTTACACCTTTTGCGAAATCCGCTCTTTTGGAAAGGGAAATATGGCTTTGGGATGTTGTTCTGAC**  
**TCCGTATTTTACACCTTTTGCGAAATCCGCTCTTTTGGAAAGGGAAATATGGCTTTGGGATGTTGTTCTGAC** 355  
  
**ETS-H / cETS-2** **ETS-I**  
ACAGAGCAAAAGGATATTTTCAGTAGC---ACAATCTCACTTTGAAAA **GGGATAAAAAGAGCCCAACACC**  
ACAGAGCAAAAGGATATTTTCAGTAGCACAACAATTTCACTTTGAAAA **GGAAAAAAGAAAAACC**-----  
ACAGAGCAAAAGGATATTTTCAGTAGCACAACAATTTCACTTTGAAAA **GGAAAAAAGAAAAACC**----- 418  
CTACTTCTCCCGCCTCCTCATGCGAGAGCTGAGGGATAGGGCACCCAGGGA-----GCTTGCTG---  
-----ATTACCCACCTTGGAG-GCAGAACCCTGAAT-GGGCA-CCAAGGACCCCTGCTCCAGGGT  
-----ATTACCTACGCTAGA-----ACAGAACCCTTGTCCAG----- 454  
  
**ETS-J** **ETS-K**  
TGCCCTACCCAGGAAGCTGTGAAAAATAT **TGTTCTTTGATTTTGGGGTTTCCCGCTGTAGGGCTTC**  
CTCTAGCCTGGG-----AGCTTTCTTTC-----TTTTT-CTCTTTTTCGATTTTACCTCTT  
TTCTCGAACAGAAA-----ACTTCCCTTTAAATTTT---TCTTTTTTTCGATTTTACCTCTT 513  
  
**ETS-L** **ETS-M**  
**CTCCCTTCCC**-----  
**TTCCCTTTCCCCTCCCTATCTGCCTCCAAGACCCTGGGATATCTTAACATCCTTCTATTGT-CCCCTT**  
**TTCCCTTTCCCCTCCCTATCTGCCTCCAAGACCCTGGGATATCTTAACATCCTTCTATTGT-CCCCTT** 582  
TTTTGAATACTATCAGGCCCTGCACATGCACACACGTAGGGCAGCTACGTAGCGGGGCTTTGGGTCCC  
TTTGAATGCTATCAAGCCCCTGCACATGCACACACCCAGGAGACTAAGTAGCAAGATTCTGGGACCC 651  
  
TCTGGCCTGTTCTTGCTGGCAGGCGGGGTCATCTGGATAACTGGGCTGATTGGTTGGCTGATCACCAT  
TCTGGCCTGTTCTTGCTGGCAGGTTAATCTAGATAATTAGAGT-----GTGAAGTACCACCAT 715  
  
CATCACAGCCAAAGAGGACATTGGCCAGCCGTCA-  
AGTCACAATAAAGAGAGAGTTGG-CAGCAGTCAACTCTCTGAATCAGTTGGCTTTCTGAATCAGG 765  
  
TTCTCTGACCAAAGCCCTTTCTG 807

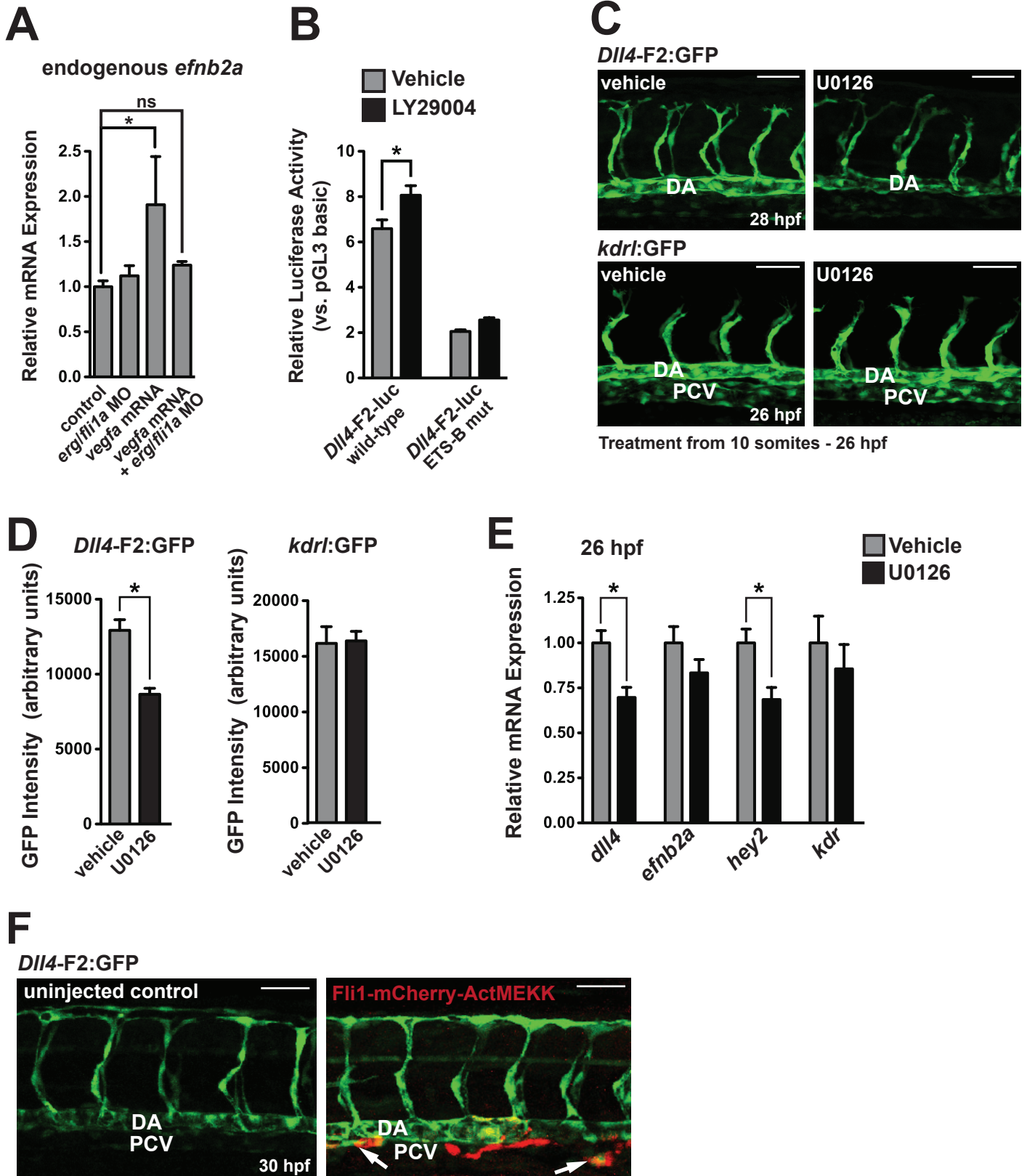
**B****C****D**











## Supplemental Figure Legends

**Figure S1 (Related to Figure 1): Wnt/ $\beta$ -Catenin signaling is not active in early arteries and does not regulate early *Dll4* expression.** (A) Conservation between murine and opossum *Dll4* with location of fragment 1 (F1) indicated. Transgenic analysis of F1-*lacZ* (E9.5) is below. (B) Representative whole-mount F1-*lacZ* transgenic embryo. (C) Whole-mount (left) and transverse sections (right) of *BAT-gal* embryos at E8.5 (n=5) and E9.5 (n=4). Dorsal aorta (arrow); cardinal vein (caret). (D) Whole-mount (left) and zoomed-in (right) *Axin2-d2EGFP* embryos at E8.5 (n=6) and E9.5 (n=8). (E) Whole-mount (left) and transverse sections (right) of *Axin2<sup>nlacZ/+</sup>* embryos at E8.5 (n=3) and E9.5 (n=5). (F) Vascular patterning in endothelial-specific *Ctnnb1* ( $\beta$ -catenin) loss-of-function (ECKO) embryos was normal, as visualized by Cre-mediated recombination of a GFP reporter allele (*Rosa26-mTomato-lox-stop-lox-mGFP [mTmG]*) (left). The dorsal aorta (arrow) and cardinal vein (caret) are indicated. A zoomed-in view (right) of the brain vasculature demonstrates a less remodeled vascular plexus (indicated by arrows) in the ECKO (n=7) embryonic brain compared to control (n=10) embryos. (G) *Dll4* in situ hybridization indicates normal expression in the dorsal aorta (arrow) of *Ctnnb1* ECKO embryos (n=4). (H) No defects in arteriovenous morphology in *Ctnnb1* null (n=5) embryos were observed, as assessed by ink injection (as ink filled the entire dorsal aorta (arrows)) and H&E histology of serial cross-sections through the rostral and caudal planes of the dorsal aortae and cardinal veins. Dorsal aorta (arrow); cardinal vein (caret). Scale bars: 500  $\mu$ m (B-H, whole-mount), 100  $\mu$ m (C-H, sections and zoom ins).

**Figure S2 (Related to Figure 3): MEF2C and RBPJk bind to the F2 enhancer, and over-expression of NICD in the endothelium can drive F2 expression in the vein, while MEF2C is dispensable for early arterial *Dll4* expression.** (A) Recombinant MEF2C protein was used in an electrophoretic mobility shift assay (EMSA) with a radiolabelled double-stranded oligonucleotide representing the F2-6 MEF2 binding site. Lane 1 contains reticulocyte lysate without recombinant MEF2C (represented by a minus sign). MEF2C efficiently bound to the F2-6 MEF2 site (lane 2) and this binding was efficiently competed by an excess of the unlabeled wild type F2-6 MEF2 element (lane 3), but not by an excess of a mutant form of this site (lane 4). (B) The F2-*lacZ* enhancer was crossed into the *Mef2c<sup>+/-</sup>* background, and wild-type and homozygous mutant embryos were stained for X-gal at E8.5, 9.0, and E9.5. No difference in enhancer activity was observable in mutant embryos compared to wild-type (*Mef2c<sup>+/+</sup>*) littermates at early stages of vascular development (i.e. E8.5-E9.0) (n  $\geq$  5 for each genotype). The dorsal aorta is indicated by arrows. Scale bars = 500  $\mu$ m (C) Expression of *Dll4* mRNA was examined by in situ hybridization in *Mef2c<sup>+/+</sup>* and *Mef2c<sup>-/-</sup>* embryos. No difference in expression was noted at E8.5 (n=3 for each genotype). Scale bars = 500  $\mu$ m (D) NICD was over-expressed in the endothelium via Tie2-Cre-mediated activation of a *R26<sup>N1CD</sup>* allele. Whole-mount images (left; scale bar = 500  $\mu$ m) and sections (right; scale bar = 100  $\mu$ m) are shown. The presence of an arteriovenous malformation (AVM) is indicated by an asterisk and the dorsal aorta (arrow) and cardinal vein (caret) are also indicated. Expression of F2 was expanded into the cardinal vein in Notch over-expression embryos. (E) EMSA showing RBPJk binding to a probe corresponding to the F2-6 RBPJk site. Binding was competed by an excess of unlabeled wild-type but not RBPJk mutant probe.

**Figure S3 (Related to Figure 4): The *Dll4* F2 enhancer contains multiple ETS binding sites.** (A) ClustalW analysis of the 802-bp *Dll4* F2 evolutionarily conserved region (ECR), comparing mouse, human, and opossum sequences. The region contains 9 perfectly



conserved ETS consensus (GGA(A/T)) sequences (red boxes). Murine F2 contains a total of 14 ETS sites, with five more non-conserved sites (blue boxes). The minimal 36-bp enhancer (F2-6) is highlighted (yellow box). Asterisks denote conserved nucleotides across all three species. **(B)** Recombinant ETS1 DNA-binding domain (DBD) was used in EMSA with radiolabelled probe encompassing a confirmed ETS-binding site from the *Mef2c* F7 enhancer. Lane 1 contains reticulocyte lysate lacking ETS1 DBD. ETS1 DBD bound the bona fide ETS-binding site in the control probe (*Mef2c* F7) (lane 2) and this specific binding was competed away by unlabeled control probe (lane 3), but binding was not competed by a control probe with a mutated ETS site (lane 4). Unlabeled probes corresponding to each of the potential ETS sites in the *Dll4* F2 enhancer were used as competitors for ETS1 DBD binding to the control probe (lanes 5-18). The *Dll4* F2 sites competed for ETS DBD binding to varying degrees. Probes encompassing ETS-B, ETS-D, ETS-H, ETS-I, ETS-J, and ETS-L competed most efficiently (lanes 8, 10, 13, 14, 15, 17, respectively). In addition to the GGA(A/T) core, ETS-B and ETS-H possessed (or overlapped with) canonical ETS sites (cETS). cETS-1/ETS-B was a consistent competitor (lanes 5 and 8), and directly bound the ETS1-DBD (panel C), but cETS-2 (lane 6) and ETS-H (lane 13) did not compete consistently, and they did not bind the ETS1-DBD directly (data not shown). **(C)** EMSA showing binding of ETS1 DNA binding domain (DBD) to the ETS-B site of F2-6. Binding was competed by an excess of unlabeled wild-type but not ETS-B mutant probe. **(D)** EMSA was performed using F2 probe and recombinant ETV2 protein. Wild-type F2 sequence effectively competed for ETV2 binding, but this competition was lost when the ETS-B site was mutated.

Figure S4 (Related to Figure 4): Analysis of ERG gain- and loss-of-function phenotypes.

**(A)** Injection of high doses of *ERG* mRNA (400 pg) in zebrafish embryos resulted in enhanced F2:GFP expression at the 20-somite stage. Premature sprouting of intersomitic vessels (arrows) was also observed. Cells were present ventral to the dorsal aorta that express F2:GFP. These may be ventrally sprouting posterior cardinal vein cells. Scale bar = 50  $\mu$ m. **(B)** Wild-type (n=2) and *Erg*<sup>Ex4/Ex4</sup> (n=2) embryos (E9.5) were stained with PECAM antibodies and confocal microscopy was utilized to observe vascular patterning. The dorsal aorta (arrow) was present and morphologically normal in *Erg* knock-out embryos. Scale bars = 500  $\mu$ m (wholemout) and 110  $\mu$ m (zoom ins). **(C)** Section in situ hybridization at E8.5 reveals reduced *Efnb2* mRNA in the dorsal aorta (arrows) in *Erg* knock out embryos (n=2) compared to wild-type littermates (n=2). Sections are counter-stained with nuclear fast red. Scale bar = 100  $\mu$ m. **(D)** Histology of serial cross-sections through wild-type (n=3) and *Erg* knock-out embryos (E9.5) (n=2) did not reveal gross morphological defects in arteries or veins. Dorsal aorta (arrow); cardinal vein (caret). Scale bar = 100  $\mu$ m.

Figure S5 (Related to Figure 5): Regulation of F2 enhancer activity by Vegf in mouse embryos and regulation of ETS factors by Vegf at early stages of zebrafish embryogenesis.

**(A)** F2-lacZ expression in the anterior DA (asterisk) is reduced in *Smoothed*<sup>-/-</sup> (*Smo*) embryos (*Smo*<sup>+/+</sup>, n=10; *Smo*<sup>-/-</sup>, n=3) at E8.25 and absent by E8.5 (*Smo*<sup>+/+</sup>, n=8; *Smo*<sup>-/-</sup>, n=4). CC, cardiac crescent. Dorsal aorta (arrows). F2 activity was abolished in *Vegfr2*<sup>-/-</sup> embryos (*Vegfr2*<sup>+/+</sup>, n=12; *Vegfr2*<sup>-/-</sup>, n=2). Scale bar = 500  $\mu$ m. **(B)** Biochemical fractionation of untreated and VEGF-treated (20 minutes) BAEC was performed and localization of ERG was analyzed. Sin3a and GAPDH were utilized as markers for nuclear and cytoplasmic protein expression, respectively. No difference in ERG localization was observed upon VEGF treatment. **(C)** Immunofluorescence of E9.5 mouse embryonic tissue for ERG (green) shows that endothelial cells, marked by

PECAM/CD31 (red), in the dorsal aorta (arrow) have stronger nuclear (DAPI) ERG expression and are more often expressing ERG than the vein (caret). Scale bar = 110  $\mu\text{m}$ . **(D)** Various ETS factors that are enriched in expression in endothelial cells (black bars) and *dll4* (white bar) were measured by qRT-PCR in control or *vegfa* morpholino-injected embryos at the 20-somite stage. *kdr* expression (gray bar) was used to assess the amount of endothelium. Data is presented as expression in *vegfa* morphants compared to control embryos (n=3; mean  $\pm$  SEM). \* indicates a significant difference in expression between *vegfa* morphants and controls. **(E)** Detailed assessment of expression kinetics (qRT-PCR) were performed in control and *vegfa* morphants. A representative experiment is shown. *kdr* and *etv2* expression was not altered by knock-down of *vegfa*, while *elk4*, *ets1a*, *erg* and *fli1a* were down-regulated in *vegfa* morphants.

Figure S6 (Related to Figure 6 and Figure 7): The F2 enhancer and endogenous *Dll4* expression are regulated by Vegf/MAP kinase signaling. **(A)** From the experiment shown in Figure 6C,D, induction of Vegfa-inducible *efnb2* was also inhibited in embryos injected with *erg/fli1a* morpholinos. Shown is qRT-PCR from 5 individual embryos per group (mean  $\pm$  SEM). \* indicates a significant difference by 1-way ANOVA. ns, not significant. **(B)** F2-luciferase activity was enhanced upon inhibition of PI3 kinase signaling (LY29004 treatment) in BAEC. The activity of F2-luciferase was decreased, and the responsiveness to PI3K inhibition was lost, when the *ETS-B* site was mutated. Shown is a representative experiment, triplicate determinations (mean  $\pm$  SEM). **(C)** F2:*GFP* or *kdrl*:*GFP* embryos were treated the MAP kinase inhibitor, U0126, starting at the 10-somite stage, and imaging was performed at 26 or 28 hpf. F2:*GFP* expression was decreased in the presence of U0126, but *kdrl*:*GFP* was unaffected. **(D)** Quantification of (C) is shown (n=4 per group; mean  $\pm$  SEM). **(E)** Expression of endogenous *dll4*, *efnb2a*, *hey2* and *kdr* was assessed by qRT-PCR (n=5-10 individual embryos; mean  $\pm$  SEM). **(F)** Embryos were injected with a construct that drives expression of constitutively active MEKK in the endothelium (Fli1-mCherry-ActMEKK). In embryos with expression of the construct in the vein, F2:*GFP* expression was also observed in venous cells (arrows).

## Supplemental Experimental Procedures:

### Bioinformatic analyses, cloning, and mutagenesis

Mouse, human, and opossum sequences were compared using ECR Browser (Ovcharenko et al., 2004), BLAST (Altschul et al., 1990) and VISTA (Mayor et al., 2000). The *Dll4* F1 fragment spanned 5,135 bp upstream of the GGG preceding the start codon in exon 1 (Chr2:119321006-119326140) and was cloned by PCR from a BAC (bMQ 132j23) containing mouse *Dll4*: forward, 5'-GGATCCTGTTGCTGCAGGCCCTAGACACTC, and reverse, 5'-GCGGCCGCCCTTG GGGTGTCTCTCCACTCC. A BamHI site was added to the forward primer and a NotI site was added to the reverse primer. The PCR fragment was purified, and cloned into Topo-XL. Upon verification by DNA sequencing, the insert was subcloned, via BamHI and NotI, into pENTR1a.

The 802-bp *Dll4* F2[1–802] fragment (Chr2:119327120-119327921) was generated by PCR using the following forward and reverse primers: 5'-ATCGGGGGATCCAGTATCTAACTTCTCGGCCACAGG-3', and 5'ATCCGCGGCCGCGCAGAAAGAGGCTTTGGTCAGAGA-3'. The underlined sequences are homologous to murine *Dll4*. The primers contained BamHI and NotI on the forward and reverse primers, respectively, and were sub-cloned into pENTR1a (Invitrogen). *Dll4*-F2-pENTR1a was digested with EcoRI and NotI, deleting an internal fragment of 504 bp, and the remaining 2,580 bp plasmid was gel extracted, blunt-end filled, and ligated to itself and transformed to generate the F2-2 plasmid. The F2-3 fragment was constructed by digesting F2-pENTR1a with BamHI and EcoRI, releasing a 304 bp fragment. The 2,780 bp backbone was gel extracted, blunt-end filled, and ligated to itself and transformed. F2-4 was amplified from a BAC containing the *Dll4* locus by PCR using the following primers: 5'-ATCGGGGGATCCGCACAATTGCGTTTCCTGCGGG and 5'-ATCCGCGGCCGCGGTTTTTCTTTTTCTTTTCAAGTGAG and cloned into pENTR1A via BamHI and NotI.

F2-6(3X) was directly synthesized (IDT) with 36-bp of *Dll4* repeated in triplicate (underlined), flanked 5' by attB1 and BamHI and 3' by NotI and attB2. F2-6(3X): 5'-ACAAGTTTGTACAAAAAGCAGGCTGGATCCGCGTTTCCTGCGGGTTATTTT TGGCGTGGGAACGCGGCGTTTCCTGCGGGTTATTTTGGCGTGGGAACGCG GCGTTTCCTGCGGGTTATTTTGGCGTGGGAACGCGGCGGCGCCGC CCCAGCTTTCTTGTACAAAGTGGT-3'. This was annealed, and duplexed DNA was recombined into pDonor-221 by a BP reaction to generate *Dll4*-F2-6(3X)-p221 for subsequent LR reactions.

The deletion construct *Dll4*-F2 $\Delta$ 2 [ $\Delta$ 1482-1518] was generated by a 3-way Cold Fusion (SSI) ligation of linearized pENTR1a with two purified PCR products flanking the 5' and 3' ends of a 36-bp core in F2 (deleting the ETS, MEF2, RBPJk, and E2F sites). The 5' flanking fragment was amplified using the following primers: 5'-AACCAATTCAGTCGACTGAGTATCTAACTTCTCGGCCACAGG (homology to pENTR1a underlined), 5'-GGATCCGCGGCCGCGGATCCAATTGTGCTCTGAGTC CAGGCAGC (polylinker underlined). The 3' half of F2 $\Delta$ 2 was amplified using primers: 5' GGATCCGCGGCCGCGGATCCGGGAGCGCGGCGGTGAGAAAGG (linker homology underlined) and 5'-GGTCTAGATATCTCGAGTGCGGCCGCAGAAAGAGGCTTTGG TCAGAGA (pENTR1a homology underlined). PCR replaced the 36-bp core with an internal BamHI-NotI-BamHI polylinker. After confirmation by sequencing, the intervening sequence between the 5' and 3' fragments was removed by digestion with BamHI, the backbone was purified and ligated to generate F2 $\Delta$ 2. F2 $\Delta$ 2 was digested with BamHI and EcoRI, end-filled, and the backbone purified and ligated to generate F2 $\Delta$ 1 [ $\Delta$ 1482-



1598]. F2Δ2 was digested with BamHI and NotI, end-filled, and the purified backbone ligated to itself to generate F2-5 pENTR1a.

To generate mutant constructs, the desired mutations validated by EMSA (see below) were engineered into either F2-6(3X)-pDONR-221 or F2-pDONR-221. For F2-6(3X), ultramer oligos with the desired mutation were synthesized (IDT), just as for wild-type F2-6(3X), annealed, and duplexed DNA was recombined into pDONR-221 via a BP reaction. Plasmids with the desired transcription factor binding mutation within F2 were directly synthesized (IDT). The inserts were then amplified from the synthetic plasmids by PCR with attb1 and attb2 sequences in the 5' and 3' oligos, respectively (5'-ACAAGTTTGTACAAAAAAGCAGGCTGGATCCAGTATCTAACTTCTCGG CCACAGG; 5'-ACCACTTTGTACAAGAAAGCTGGGGCGGCCGAGAAAGAGGCTTTGGTCA GAGA) (homology to *Dll4* F2 is underlined). These inserts were purified, and recombined into pDONR-221 via a BP reaction, and sequenced to confirm the mutation. All mutant clones were then shuttled into pGL3pro-DV (a modified version of pGL3-promoter-luciferase containing a Gateway Destination Vector), tol2-E1b-GFP, and *hsp68-lacZ* destination vectors by LR recombination reactions.

### **Generation of transgenic mice**

The pBSK-AUG-β-gal plasmid was digested in the polylinker using a blunt-cutter (SmaI) and an RFA "B" Gateway cassette (Invitrogen) was inserted 5' to the promoterless AUG-*lacZ* reporter to make a destination vector (pBSK-AUG-*lacZ*-DV). A similar strategy was used to modify pBSK-*hsp68-lacZ* (Kothary et al., 1989), to obtain pBSK-*hsp68-lacZ*-DV. Upon LR recombination with DONR or entry clones and destination reporter plasmids, the final vectors were restriction mapped and verified by DNA sequencing. Transgenic *lacZ* reporter fragments were generated by gel purifying Sall fragments from recombined AUG-*lacZ*-DV or *hsp68-lacZ*-DV plasmids. Pronuclear injection of transgenic fragments was performed at the Gladstone Institute, or by Cyagen Biosciences (Gunzu, China). The presence of *lacZ* transgenes in embryo yolks sacs was detected by PCR using primers specific for the transgene, or for *lacZ* (5'-TCGTTGTGCATAAACCGACT; 5'-GACCATTTTCAATCCGCACCT). All experiments using mice were reviewed and approved by the UCSF Institutional Animal Care and Use Committee and complied with all institutional and federal guidelines.

### **Genotyping and mice used**

*Dll4<sup>lacZ/+</sup>* (*Dll4<sup>tmJrt</sup>*) (Duarte et al., 2004) cryopreserved embryos were purchased from the Canadian Mouse Mutant Repository (CMMR) and implanted into CD31 females. *β-catenin* (*Ctnnb1*) (Brault et al., 2001), *Axin2-d2EGFP* (Jho et al., 2002), *BAT-gal* (Maretto et al., 2003), *Axin2<sup>lacZ/+</sup>* (Lustig et al., 2002), *Rbpjk* (Han et al., 2002), *Erg* (Vijayaraj et al., 2012), *Mef2c* (Vong et al., 2005), *Smo* (Zhang XM et al., 2001), *Vegfr2* (Ema et al., 2006), *R26<sup>N1CD</sup>* (Murtaugh et al., 2003), and *Tie2-cre* (Braren et al., 2006) mice have all been described previously. *Mef2c<sup>flox/+</sup>*, *Ctnnb1<sup>flox/+</sup>* and *Rbpjk<sup>flox/+</sup>* mice were each mated to *Mef2c*-AHF-Cre females (which acts as a universal deleter strain in the female germ line) to generate offspring with global null (deleted, or del) alleles. Matings were designed so that only one LoxP-flanked (floxed) allele needs to undergo recombination to create endothelial-specific knockout mice. In the first cross, heterozygous del mice were bred to a *Tie2-Cre* transgenic male (to avoid female germ line activity of *Tie2-Cre*) (de Lange et al., 2008), and the resulting male offspring that inherited the del allele and *Tie2-Cre* transgene were then mated to females homozygous for the floxed allele to generate endothelial-specific loss-of-function (ECKO) embryos. All floxed alleles were maintained in a *R26<sup>mTmG/mTmG</sup>* (Muzumdar et al., 2007) background. Endothelial-specific activity of *Tie2-Cre* was confirmed by GFP immunofluorescence

within the endothelium. Where appropriate, the *F2-hsp68-lacZ* transgene was maintained in males. Genotyping for all alleles was performed by PCR (see table below for primer sequences).

### **Electrophoretic mobility shift assay (EMSA)**

EMSA was performed as before (Dodou et al., 2003). Briefly, double-stranded oligonucleotides containing 5' and 3' GG overhangs were labeled with <sup>32</sup>P-dCTP, using Klenow to fill in overhanging 5' ends, and purified on a non-denaturing polyacrylamide-TBE gel. Binding reactions were pre-incubated at room temperature in modified 1x binding buffer (15 mM KCl, 5 mM Hepes pH 7.9, 5% glycerol, 0.04 mM EDTA, 0.125 mM DTT, 0.25 mM PMSF) containing recombinant protein, 1 ug of poly dI-dC, and unlabeled competitor DNA (50-fold excess, where indicated) for 10 min before probe addition. Reactions were incubated an additional 20 min at room temperature after probe addition and electrophoresed on a 10% nondenaturing polyacrylamide gel.

The DNA-binding domain of murine ETS-1 in pCITE-2A (Novagen) containing the 85 amino acids ETS domain but no auto-inhibitory domain, efficiently binds *bona fide* ETS sites (Nye et al., 1992), and has been described before (De Val et al., 2004). The full-length ETV2-pCITE-2A (De Val et al., 2008) and pCDNA3.1-RBPJk (Liang et al., 2002) have been described before, and the pCITE-2B-MEF2C cloning will be detailed elsewhere. All recombinant proteins were transcribed and translated using the TNT Coupled Transcription–Translation system (Promega) according to the manufacturer's instructions.

The ETS1 control (*Mef2c*-F7 ETS-A) and mutant control probe sequences have been described previously (De Val et al., 2004) and were: control, 5'-gctcagagaaggaagtggagagt-3'; mutant, 5'-gctcagagaagccttggtggaggtt-3'. The sequences of the competitor oligonucleotides encompassing the ETS sites from the *Dll4* F2 enhancer were:

- 1) ETS-A, 5'-GGTGGACGCTCGGATTCCGCTCGCTGCCTG-3'.
- 2) ETS-B/cETS-1a site, 5'-GGGCACAATTGCGTTTTCCCTGCGGGTATTT-3';
- 3) ETS-C, 5'-GGATTTTTGGCGTGGGAACGCGGGGAGCGC-3';
- 4) ETS-D, 5'-GGCTGACGGGCCTCTTCCCTGTATTTTACAC-3';
- 5) ETS-E(/F), 5'-GGACCTTTTGCGAATTCCGCTCCTTTGGAAA-3';
- 6) ETS-E/F/G, 5'-GGTTCCGCTCCTTTGGAAAGGGAATAATGG-3';
- 7) ETS-H /cETS-1b site, 5'-GGTTCTGACACAGAGGAAAAGGATATTTCA-3';
- 8) ETS-I (NFATc1), 5'-GGTCACTTTGAAAAGGAAAAAGAAAAACCA-3';
- 9) ETS-J, 5'-GGGAACCAGAAAACCTTCCCTTTAAATTT-3';
- 10) ETS-K, 5'-GGTTTTTTCTTTTTTTCCATTTTGACCTCT-3';
- 11) ETS-L/M-#1, 5'-GGTTTTGACCTCTTTTCCCTCTTTCCCTCC-3';
- 12) ETS-L/M-#2, 5'-GGCTCTTTTCCCTCTTTCCCTCCGTATCTG

cETS-1b, 5' GGTCTGACACAGAGGAAAAGGATATTTACCAGCACAAC  
cETS-1a, 5' GGCAGAGCACAATTGCGTTTTCCCTGCGGGTATTTTTGGCG  
cETS-1a mut, 5' GGCAGAGCACAATTGCGTTTTTGGCGGGTATTTTTGGCG  
The sequences for the ETS mutant sites were identical to the mutagenic primers described above. For the ETS-6X mutant, ETS sites B, D, H, I, J, and L were all mutated in cis as described above.

The sequences of the RBPJk sites within *Dll4* F2 were: *Dll4* F2 RBPJk, 5'-GGGGTATTTTTGGCGTGGGAACGCGGGGAGCGC-3'; *Dll4* F2 RBPJk Mutant, 5'-GGGGTATTTTTGGCaaccctACGCGGGGAGCGC-3'. The sequences of the MEF2 sites within *Dll4* F2 were: *Dll4* F2 MEF2, 5'-GGATTGCGTTTCCCTGCGGGTATTTTITGGCGTGGGAACGCGGGGAGCG-3'. *Dll4* F2 MEF2 mutant, 5'-GGATTGCGTTTCTGCGGGTATtggcTGGCGTGGGAACGCGGGGAGCG.

### **Cloning of pCS2-V5-ERG**

Human ERG open reading frame (ORF) was amplified from plasmid DNA (IMAGE clone #6052140) and a XhoI site, kozak sequence, and V5 epitope tag were added to the 5' end, while an XbaI restriction site was added to the 3' end (5'-ATCCCTCGAGGCCAC CATGGGTAAGCCTATCCCTAACCCCTCCTCGGTCTCGATTCTACGATGGCCAGCA CTATTAAGGAAGC; 5'-GAATTCTAGATTATTAGTAGTAAGTGCCCAGATGAGAAGGC) and cloned into pCRII-TOPO-zero blunt. The insert was then subcloned into the pCS2 expression vector using XhoI and XbaI.

### **In situ hybridization**

The murine *Dll4* riboprobe was from Janet Rossant (Duarte et al., 2004), and the *Efnb2* riboprobe, spanning the second to fifth exon of the *Efnb2* cDNA, was from Jeffrey Bush and Ace Lewis (UCSF). Embryos were processed as previously described (Wythe et al., 2011). CD31 immunostained embryos were embedded in 1% low melt agarose in PBS, and cleared in *Clear*<sup>T2</sup> (Kuwajima et al., 2013) prior to imaging. Wholmount lacZ and indirect immunofluorescent images were obtained using a Leica dissecting microscope and camera with the Leica LAS Montage extended focus function. Confocal images were obtained on a Nikon ECLIPSE Ti 2000 confocal microscope with a Yokogawa CSU-X1 spinning disk and Hamamatsu ImagEM CCD camera. Images were processed using Velocity software (Perkin Elmer).

### **Zebrafish experiments**

The *Tg(Dll4-F2-E1b:GFP)* line was generated by injecting a Tol2 construct containing the mouse *Dll4* F2 sequence (see below for details) into 1-cell embryos. Morpholinos against *vegfa* (5'-CTC GTC TTA TTT CCG TGA CTG TTT T (Ober et al., 2004), 2.5 ng), *rbpj* (5'-CAA ACT TCC CTG TCA CAA CAG GCG C (Siekman and Lawson, 2007), 2.5 ng), *erg* (5'-AGA CGC CGT CAT CTG CAC GCT CAG A, 8 ng) and *fli1a* (5'-TTT CCG CAA TTT TCA GTG GAG CCC G (Liu and Patient, 2008), 2ng) were injected into 1-2 cell embryos. For MAPK inhibition studies, embryos were dechorionated and treated with 20  $\mu$ M U0126 (Invivogen) or DMSO from the 10-somite stage to 28 hpf. Vibratome sectioning, embedding of live and fixed embryos, and confocal analyses were performed as before (Fish et al., 2011). In some experiments indirect immunofluorescence of *Tg(Dll4-F2:GFP)* was performed as described previously (Fish et al., 2011). Quantification of GFP intensity was performed using ImageJ. For transgenesis experiments, enhancer elements were subcloned into pDONR 221 (Invitrogen), then recombined into a Destination Vector (Invitrogen) containing two tol2 sites flanking a gateway recombination site and a minimal promoter (E1b) driving EGFP (Birnbaum et al., 2012). 25-40 pg of Tol2-containing DNA plasmids and 35-75 pg of transposase mRNA were injected into the cell of 1-cell stage embryos. pCS2-mCherry, pCS2-transposase, pCMV-Sport6-ERG, pCS2-Vegfa<sub>121</sub> and pCS2-Vegfa<sub>165</sub> (both from Nathan Lawson) (Lawson et al., Dev Cell, 2002) were linearized and capped mRNA was transcribed using the SP6 mMessage mMachine Kit (Ambion). 200 pg or 400 pg of *ERG* mRNA were injected for rescue or phenotypic analyses, respectively. 300 pg of *Vegfa*<sub>121</sub> and 100 pg of *Vegfa*<sub>165</sub> were injected together. When *Vegfa*<sub>121/165</sub> mRNA and *erg/fli1a* morpholinos were injected in combination, 4 ng of *erg* morpholino and 1 ng of *fli1a* morpholino were used. In some experiments, 100 pg of *mCherry* mRNA was co-injected to determine which embryos were successfully injected with Tol2 constructs, or as a control mRNA. 100 pg of pTol-*fliepcherryactMEKK* (Covassin et al., 2009), which drives endothelial-specific expression of mCherry and constitutively-active mitogen activated



protein kinase 1 (MAP2K1) (a kind gift of Nathan Lawson), was co-injected with transposase mRNA.

#### **Quantitative reverse-transcriptase PCR (qRT-PCR)**

RNA was isolated from cultured cells or pooled zebrafish embryos using Trizol (Invitrogen). RNA from individual zebrafish embryos was isolated using RNeasy Mini Kit (Qiagen). Mouse embryos were snap frozen and RNA was isolated using the RNAqueous Micro Kit (Ambion). RNA was reverse transcribed using the high-capacity cDNA reverse transcription kit (Applied Biosystems). qRT-PCR was performed using a Roche Lightcycler 480® with LC 480 SYBR Green I Master Mix (Roche) or LC 480 Probes Master Mix (Roche). Data were normalized to Tata box binding protein (*TBP*) or to *Gapdh* (mouse experiments) using the Delta-Delta Ct method. Sybr green primers are listed in the table below. The following Assay On Demand probes were used for mouse genes: *Pecam1* (Mm01242576\_m1), *Dll4* (Mm00444619\_m1), *Notch1* (Mm00435249\_m1), *Notch4* (Mm00440525\_m1), *Cxcr4* (Mm01292123\_m1), *Efnb2* (Mm01215897\_m1), and *Gapdh* (4352932) (Applied Biosystems).

Primers used for qRT-PCR and ChIP analyses: Species of the gene and sequences of primers are indicated. Primers used for ChIP analyses are indicated as 'ChIP' primers.

Gene	Forward Primer 5'-3'	Reverse Primer 5'-3'
human <i>DLL4</i>	TGCGAGAAGAAAGTGGACAG	ACAGTAGGTGCCCGTGAATC
human <i>NOTCH4</i>	CTGGCTGTCCACCCTCAT	GAGCTGGAGGACGAGAAGAG
human <i>TBP</i>	TCGGAGAGTTCTGGGATTGT	CACGAAGTGCAATGGTCTTT
bovine <i>COUP-TFII</i>	CGGATCTTCCAAGAGCAAGT	TCAGAGAGACCACAGGCATC
bovine <i>DLL4</i>	GGCAATGCACTTGTGATGA	GGCGACAGGTGCAGGTAT
bovine <i>EFNB2</i>	CCAGACAAGAGCCATGAAGA	TGGTTTGACAAAGGGACTTG
bovine <i>EPHB4</i>	AGTGGCTTCGAGCCATTAAG	AGCAGGTCCTCAGTGGAGAT
bovine <i>HES1</i>	TGGAAATGACAGTGAACACC	GTCACCTCGTTCATGCACTC
bovine <i>NOTCH1</i>	AAACACGTGGAGGCTGCT	ACCTTGGCGGTCTCGTAG
bovine <i>NOTCH4</i>	TGGTTGAAGAACTGATTGCAG	CATCCTGTGCGTCTTTATCG
bovine <i>TBP</i>	GGTTAGAAGGCCTTGTGCTT	GGAGAACAAATTCTCGGTTTGA
zebrafish <i>dll4</i>	GGACAAATGCACCAGTATGC	GTTTGCGCAGTCGTTAATGT
zebrafish <i>efnb2a</i>	CAGTTACCCTCCCAAACACC	CTCCCTTATCTTCCCATGA
zebrafish <i>elf1</i>	CTTCTGCAGACGGTTCATGT	GTCATTGGACCTCCTCCTTG
zebrafish <i>elf2a</i>	CCTCAGGACAAGATGCCTTT	TTCTGACCCTGTGTGCGTCAT
zebrafish <i>elf2b</i>	GTTCAGCGCACAGTAATGGT	ACCGTGGAGATCTTCTGTCC
zebrafish <i>elk4</i>	ATTTCTGGAGCACGCTGAG	TGTGTTGGTGCCGTCTAAAT
zebrafish <i>erg</i>	AGATTTTAGGGCCGACCAG	TGATGCAGGACGAGTTGC
zebrafish <i>ets1a</i>	AGCTCCAGCTTCCAGGAGT	TATTCAGACGGAGGGACACA
zebrafish <i>ets2</i>	CCACCTGTCAGAGCATCATC	TCTTGGGCTTGTTCTTCTC
zebrafish <i>etv2</i>	CCTGCTTTGCTGCTCTGCTTC ATAC	TCCCACAATGGACACCAGCAGC
zebrafish <i>fli1a</i>	TGACGACCAATGAGAGGAGA	CGTGTGATCTCCTGAAGAC
zebrafish <i>fli1b</i>	CCAAGCATTAGGTTCCATCA	TCGGAAAGCAACTCCAGTAA
zebrafish <i>kdr</i>	CTCACCTTCAACGTGGCTAA	TGATGTTCAAGGTTGGAGGA
zebrafish <i>kdr1</i>	AAGGCTTCTTCACTCTTCACG	GAGTGTGAGTGTCCCACCAA
zebrafish <i>tel (etv6)</i>	CACGAGCGCTCAGACACTAC	CTGACTCCAGATGCTCCAGA
zebrafish <i>tbp</i>	TGGGTTTCCCTGCCAAATTCTT	GGAAATAACTCCGGTTCATAGCTGC
human/bovine <i>DLL4</i> intron 3 (F2) ChIP	GTTTCCTGCGGGTTATTTTT	CTTTCCAAAGGAGCGGAAT
human <i>DLL4</i> exon 11 ChIP	CCCATGCCTCCAACACTACTGT	GGGTAGACGGACATTCTTGC
bovine <i>DLL4</i> exon 11 ChIP	GGAAATTCTGGTGAGGGAGA	GAAGATCGGCTTCAAGGGTA
bovine <i>NOTCH4</i> intron 1 ChIP	TGGAGACATGGGAAAGTCAA	GAGGTGAATGGCTGAAACAC

Primers used for genotyping analyses: The allele, mouse genome informatics (MGI) number, primer sequence and amplicon size for transgenic, wild-type (WT), gain-of-function (GOF) and knock-out (del) alleles are indicated.

MGI #	Allele	Forward 5'-3'	Reverse 5'-3'	Band Size
3056 400	<i>Dll4</i> <sup>lacZ/+</sup> WT allele	GGGGAATCAGCTTTTCAGGAA	CGAACTCCTGCAGCCGCAGCT	300 bp
	<i>Dll4</i> <sup>lacZ/+</sup> lacZ allele	GGGGAATCAGCTTTTCAGGAA	ACGACGTTGTAATACGAC	110 bp
	<i>Ctnnb1</i> <sup>fl/+</sup> WT/flox	AAGGTAGAGTGATGAAAGTTGTT	CACCATGTCCTCTGTCTATTC	221 bp 324 bp
2148 569	<i>Ctnnb1</i> <sup>fl/+</sup> del allele	TACACTATTGAATCACAGGGACTT	CACCATGTCCTCTGTCTATTC	500 bp
	<i>Rbpjk</i> <sup>fl/+</sup> WT allele	ACCAGAATCTGTTTGTATTTCATTAC TG	ATGTACATTTTGTACTCACAGAGATGG ATG	300 bp
	<i>Rbpjk</i> <sup>fl/+</sup> del allele	ACCAGAATCTGTTTGTATTTCATTAC TG	TCCACCATGATTTGCTTGAG	700 bp
3697 064	<i>BAT-gal</i>	CATTTCCCCAAAAACACATC	GTTTTCCAGTCACGACGTT	218 bp
3836 891	<i>Axin2-d2EGFP</i>	TCAGATTTTCGCTTTTGAAAAAGCTGCGT CG	TGTGGTCGGGGTAGCGGCTG	500 bp
3579 503	<i>Axin2</i> <sup>nlacZ/+</sup> WT allele	AAGCTGCGTCGGATACTTGCGA	AGTCCATCTTCATTCCGCCTAGC	493 bp
	<i>Axin2</i> <sup>nlacZ/+</sup> lacZ allele	AAGCTGCGTCGGATACTTGCGA	TGGTAATGCTGCAGTGGCTTG	400 bp
3603 182	<i>Mef2c</i> <sup>-/-</sup> WT allele	GTGATGACCCATATGGGATCTAGAAAT CAAGGTCCAGGGTCAG	CTACTTGTCCCAAGAAAGGACAGGAA ATGCAAAAATGAGGCA	586/ 838 bp
	<i>Mef2c</i> <sup>-/-</sup> del allele	GTGGGCTCTATGGCTTCTGAGGCGGAA AG	CTACTTGTCCCAAGAAAGGACAGGAA ATGCAAAAATGAGGCA	253 bp
5443 838	<i>Erg</i> <sup>Ex4/+</sup> del allele	TTGTTCCCACGGAGAATCCGA	TCATCGGTCAGACGATTTCATTGGCA	949 bp
	<i>Erg</i> <sup>Ex4/+</sup> WT allele	CACCTCTGTGTGGGATTCCCT	ATGATGGCCATTAAGGCTTG	542 bp
	Generic <i>lacZ</i>	GCCAAAATCACCGCCGTAAG	TCGCTGGGAATGAATCAGG	320 bp
	F2/3/4- <i>lacZ</i>	ACGGGCCTCTTCCTGTATTT	AGTGCTGCCTCTGACCTCAT	400 bp
3810 530	<i>Tie2-Cre</i>	CCCTGTGCTCAGACAGAAATGAGA	CGCATAACCAGTGAAACAGCATTGC	560 bp
2176 255	<i>Smo</i> <sup>del/+</sup> WT allele	CACCGGTGCCTAAGTAGC	CCAGCAGTACCAGCAGCAG	190 bp
	<i>Smo</i> <sup>del/+</sup> del allele	CACCGGTGCCTAAGTAGC	GCCAGAGGCCACTTGTGTAG	240 bp
3629 041	<i>Flk1</i> <sup>GFP/+</sup> WT allele	TGGAGAGCAAGGCGCTGCTAGC	CTTCCACTCCTGCCTACCTAG	322 bp
	<i>Flk1</i> <sup>GFP/+</sup> GFP allele	CCCCCTGAACCTGAAACATA	CTTCCACTCCTGCCTACCTAG	600 bp
2684 314	<i>R26</i> <sup>N1ICD</sup> WT allele	CCAAAGTCGCTCTGAGTTGTTATC	GAGCGGGAGAAATGGATATG	604 bp
	<i>R26</i> <sup>N1ICD</sup> GOF allele	AAAGTCGCTCTGAGTTGTTAT	GAAAGACCGCGAAGAGTTTG	320 bp



## Supplemental References

Altschul, S.F., Gish, W., Miller, W., Myers, E.W., and Lipman, D.J. (1990). Basic local alignment search tool. *J Mol Biol* 215, 403-410.

Birnbaum, R.Y., Clowney, E.J., Agamy, O., Kim, M.J., Zhao, J., Yamanaka, T., Pappalardo, Z., Clarke, S.L., Wenger, A.M., Nguyen, L., *et al.* (2012). Coding exons function as tissue-specific enhancers of nearby genes. *Genome Res* 22, 1059-1068.

Braren, R., Hu, H., Kim, Y.H., Beggs, H.E., Reichardt, L.F., and Wang, R. (2006). Endothelial FAK is essential for vascular network stability, cell survival, and lamellipodial formation. *The Journal of cell biology* 172, 151-162.

Brault, V., Moore, R., Kutsch, S., Ishibashi, M., Rowitch, D.H., McMahon, A.P., Sommer, L., Boussadia, O., and Kemler, R. (2001). Inactivation of the beta-catenin gene by Wnt1-Cre-mediated deletion results in dramatic brain malformation and failure of craniofacial development. *Development* 128, 1253-1264.

Covassin, L.D., Siekmann, A.F., Kacergis, M.C., Laver, E., Moore, J.C., Villefranc, J.A., Weinstein, B.M., and Lawson, N.D. (2009). A genetic screen for vascular mutants in zebrafish reveals dynamic roles for Vegf/Plcg1 signaling during artery development. *Dev Biol* 329, 212-226.

de Lange, W.J., Halabi, C.M., Beyer, A.M., and Sigmund, C.D. (2008). Germ line activation of the Tie2 and SMMHC promoters causes noncell-specific deletion of floxed alleles. *Physiol Genomics* 35, 1-4.

De Val, S., Anderson, J.P., Heidt, A.B., Khiem, D., Xu, S.M., and Black, B.L. (2004). Mef2c is activated directly by Ets transcription factors through an evolutionarily conserved endothelial cell-specific enhancer. *Developmental biology* 275, 424-434.

De Val, S., Chi, N.C., Meadows, S.M., Minovitsky, S., Anderson, J.P., Harris, I.S., Ehlers, M.L., Agarwal, P., Visel, A., Xu, S.M., *et al.* (2008). Combinatorial regulation of endothelial gene expression by ets and forkhead transcription factors. *Cell* 135, 1053-1064.

Dodou, E., Xu, S.M., and Black, B.L. (2003). mef2c is activated directly by myogenic basic helix-loop-helix proteins during skeletal muscle development in vivo. *Mech Dev* 120, 1021-1032.

Duarte, A., Hirashima, M., Benedito, R., Trindade, A., Diniz, P., Bekman, E., Costa, L., Henrique, D., and Rossant, J. (2004). Dosage-sensitive requirement for mouse Dll4 in artery development. *Genes & development* 18, 2474-2478.

- Ema, M., Takahashi, S., and Rossant, J. (2006). Deletion of the selection cassette, but not cis-acting elements, in targeted Flk1-lacZ allele reveals Flk1 expression in multipotent mesodermal progenitors. *Blood* *107*, 111-117.
- Fish, J.E., Wythe, J.D., Xiao, T., Bruneau, B.G., Stainier, D.Y., Srivastava, D., and Woo, S. (2011). A Slit/miR-218/Robo regulatory loop is required during heart tube formation in zebrafish. *Development* *138*, 1409-1419.
- Han, H., Tanigaki, K., Yamamoto, N., Kuroda, K., Yoshimoto, M., Nakahata, T., Ikuta, K., and Honjo, T. (2002). Inducible gene knockout of transcription factor recombination signal binding protein-J reveals its essential role in T versus B lineage decision. *International immunology* *14*, 637-645.
- Jho, E.H., Zhang, T., Domon, C., Joo, C.K., Freund, J.N., and Costantini, F. (2002). Wnt/beta-catenin/Tcf signaling induces the transcription of Axin2, a negative regulator of the signaling pathway. *Molecular and cellular biology* *22*, 1172-1183.
- Kothary, R., Clapoff, S., Darling, S., Perry, M.D., Moran, L.A., and Rossant, J. (1989). Inducible expression of an hsp68-lacZ hybrid gene in transgenic mice. *Development* *105*, 707-714.
- Kuwajima, T., Sitko, A.A., Bhansali, P., Jurgens, C., Guido, W., and Mason, C. (2013). ClearT: a detergent- and solvent-free clearing method for neuronal and non-neuronal tissue. *Development* *140*, 1364-1368.
- Liang, Y., Chang, J., Lynch, S.J., Lukac, D.M., and Ganem, D. (2002). The lytic switch protein of KSHV activates gene expression via functional interaction with RBP-Jkappa (CSL), the target of the Notch signaling pathway. *Genes & development* *16*, 1977-1989.
- Liu, F., and Patient, R. (2008). Genome-wide analysis of the zebrafish ETS family identifies three genes required for hemangioblast differentiation or angiogenesis. *Circ Res* *103*, 1147-1154.
- Lustig, B., Jerchow, B., Sachs, M., Weiler, S., Pietsch, T., Karsten, U., van de Wetering, M., Clevers, H., Schlag, P.M., Birchmeier, W., *et al.* (2002). Negative feedback loop of Wnt signaling through upregulation of conductin/axin2 in colorectal and liver tumors. *Mol Cell Biol* *22*, 1184-1193.
- Maretto, S., Cordenonsi, M., Dupont, S., Braghetta, P., Broccoli, V., Hassan, A.B., Volpin, D., Bressan, G.M., and Piccolo, S. (2003). Mapping Wnt/beta-catenin signaling during mouse development and in colorectal tumors. *Proceedings of the National Academy of Sciences of the United States of America* *100*, 3299-3304.

Mayor, C., Brudno, M., Schwartz, J.R., Poliakov, A., Rubin, E.M., Frazer, K.A., Pachter, L.S., and Dubchak, I. (2000). VISTA : visualizing global DNA sequence alignments of arbitrary length. *Bioinformatics* 16, 1046-1047.

Murtaugh, L.C., Stanger, B.Z., Kwan, K.M., and Melton, D.A. (2003). Notch signaling controls multiple steps of pancreatic differentiation. *Proc Natl Acad Sci U S A* 100, 14920-14925.

Muzumdar, M.D., Tasic, B., Miyamichi, K., Li, L., and Luo, L. (2007). A global double-fluorescent Cre reporter mouse. *Genesis* 45, 593-605.

Nye, J.A., Petersen, J.M., Gunther, C.V., Jonsen, M.D., and Graves, B.J. (1992). Interaction of murine ets-1 with GGA-binding sites establishes the ETS domain as a new DNA-binding motif. *Genes & development* 6, 975-990.

Ober, E.A., Olofsson, B., Makinen, T., Jin, S.W., Shoji, W., Koh, G.Y., Alitalo, K., and Stainier, D.Y. (2004). Vegfc is required for vascular development and endoderm morphogenesis in zebrafish. *EMBO Rep* 5, 78-84.

Ovcharenko I., Nobrega, M.A., Loots, G.G., and Stubbs, L. (2004). ECR Browser: a tool for visualizing and accessing data from comparisons of multiple vertebrate genomes. *Nucleic Acids Res* 32, W280-286.

Siekman, A.F., and Lawson, N.D. (2007). Notch signalling limits angiogenic cell behaviour in developing zebrafish arteries. *Nature* 445, 781-784.

Vijayaraj, P., Le Bras, A., Mitchell, N., Kondo, M., Juliao, S., Wasserman, M., Beeler, D., Spokes, K., Aird, W.C., Baldwin, H.S., *et al.* (2012). Erg is a crucial regulator of endocardial-mesenchymal transformation during cardiac valve morphogenesis. *Development (Cambridge, England)* 139, 3973-3985.

Vong, L.H., Ragusa, M.J., and Schwarz, J.J. (2005). Generation of conditional Mef2cloxP/loxP mice for temporal- and tissue-specific analyses. *Genesis* 43, 43-48.

Wythe, J.D., Jurynek, M.J., Urness, L.D., Jones, C.A., Sabeh, M.K., Werdich, A.A., Sato, M., Yost, H.J., Grunwald, D.J., Macrae, C.A., *et al.* (2011). Hap1, a newly identified pleckstrin homology domain protein, is required for cardiac contractility in zebrafish. *Disease models & mechanisms* 4, 607-621.